PONTIFICIA UNIVERSIDAD CATÓLICA DE CHILE
ESCUELA DE INGENIERÍA

EFFECT OF SOILING IN BIFACIAL PV MODULES AND CLEANING FREQUENCY ANALYSIS

ENRIC TOMAS GRAU LUQUE

Thesis submitted to the Office of Research and Graduate Studies
in partial fulfillment of the requirements for the degree of
Master of Science in Engineering

Advisor:
RODRIGO ESCOBAR MORAGAS

Santiago de Chile, May 2018

PONTIFICIA UNIVERSIDAD CATÓLICA DE CHILE
ESCUELA DE INGENIERÍA

EFFECT OF SOILING IN BIFACIAL PV MODULES AND CLEANING FREQUENCY ANALYSIS

ENRIC TOMAS GRAU LUQUE

Members of the Committee:
RODRIGO ESCOBAR MORAGAS
MATIAS NEGRETE-PINCETIC
PAULO AYALA
FERNANDO ANTONANZAS
CRISTIAN ESCAURIAZA

Thesis submitted to the Office of Research and Graduate Studies
in partial fulfillment of the requirements for the degree of
Master of Science in Engineering

Santiago de Chile, May 2018

" I'm smart enough to know that
I'm dumb " - Richard Feynman

ACKNOWLEDGEMENTS

First, I would like to thank my thesis advisor Rodrigo Escobar Moragas of the Mechanical Engineering Department of the Engineering School at Pontificia Universidad Catolica de Chile, that with infinite patience and disposition guided me to the proper realization of this work.

Also, I would like to thank the team, professionals and students, working on the solar research center at PUC and to the, that with good will listened and helped.

Special thanks and acknowledgment to the Energy Research Centre of the Netherlands (ECN) that provided the minimodules used on the experiment.

Finally but not least, to my father, mother and sisters who put up with all my personal development and progress through this process, alway with great support and interest in my work. For your constant love I will always be grateful.

TABLE OF CONTENTS

LIST OF FIGURES

LIST OF TABLES

ABSTRACT

Bifacial photovoltaic (PV) modules and cells can transform solar radiation into electricity from both front and rear sides, unlike traditional solar technologies which can only generate power through the front face. This ability has shown to increase electric output with various levels of increment, depending on parameters such as distance to the ground, distance between modules, and albedo. This power gain characteristic versatility has attracted the industry, gaining both commercial and research interest.

Measuring soiling effects in bifacial modules is an important milestone for the technology, since it is an important source of efficiency loss, thus relevant to the industry when evaluating and designing bifacial systems.

In this work soiling rates are measured for bifacial minimodules and compared with traditional monofacial minimodules. The experiment was carried out for a period of two months in Santiago, Chile, measuring short circuit current of the minimodules along with the irradiance in the module plane and albedo. Also, a methodology is proposed to distinguish between soiling in the front and rear sides of bifacial modules, with which a mixed integer lineal problem is designed to obtain optimum cleaning frequency under different strategies and conditions for a period of three years, from 2014 to 2016.

It is observed that soiling rate in the monofacial minimodule is 0.301%/day, meanwhile a rate of 0.236%/day was measured for the bifacial module. Also, a rate of 0.0343%/day was calculated fo the rear side of the bifacial module, roughly 8.8 times smaller that the front side rate.

Finally, several simulations where performed to see the effects of soiling rate, albedo, cleaning costs and strategy in cleaning frequency of both the front and rear sides of a bifacial PV system.

Keywords: Bifacial, photovoltaic (PV), solar, soiling, cleaning, Chile.

RESUMEN

Los módulos y celdas fotovoltaicas (PV) bifaciales pueden transformar radiación solar en electricidad tanto por la cara anterior como posterior, a diferencia de la tecnología tradicional que solo genera potencia en la cara frontal. Esta habilidad ha demostrado incrementar la generación de electricidad en diferentes niveles, dependiendo de parámetros como albedo, distancia al suelo y distancia entre módulos. Esta ganancia en energa ha atraído a la industria en los últimos aos, ganando mayor interés comercial y científico.

Medir los efectos de ensuciamiento es un importante hito para la tecnología, ya que es una fuente considerable de pérdida de eficiencia y, por lo tanto, relevante para la industria al evaluar y diseãr sistemas bifaciales.

En este trabajo, tasas de ensuciamiento son medidas para minimodulos bifaciales y comparados con tecnología tradicional. El experimento se llevó a cabo en un período de dos meses en Santiago, Chile, midiendo corriente de corto circuito junto con la radiación en el plano y albedo. Adems, se propone una metodología para distinguir ensuciamiento de la cara anterior y posterior del módulo bifacial, junto con lo cual se desarrolló un problema lineal entero mixto para obtener frecuencias de limpieza óptimas bajo diferentes estrategias y condiciones de ensuciamiento durante tres aos, entre 2014 y 2016.

Es observado que la tasa de ensuciamiento para la tecnología tradicional es de 0.301 %/día, mientras para el módulo bifacial es de un 0.236 %/día. Tambin, una tasa de 0.0343 %/día se estima para la cara posterior del modulo bifacial, cerca de 8,8 veces el ensuciamiento de la cara frontal.

Finalmente, se llevaron a cabo varias simulaciones para ver los efectos de ensuciamiento, albedo, costo de limpieza y estrategia de limpieza en la frecuencia óptima de limpieza para un sistema fotovoltaico bifacial.

Palabras Claves: Bifacial, fotvoltaico (PV), solar, ensuciamiento, limpieza, Chile.

1. INTRODUCTION

1.1. Motivation

Worldwide, electricity generation is largely dominated by fossil fuels with a participation of 66.7% in 2014, while only 6.3% belongs to renewable input without hydro (Figure 1.1). Primary energy supply gets a bigger portion of fossil fuels, with 81.1% and with only 1.4% of renewable input without hydro, and just 3.8% with it (Figure 1.2). This dominance of fossil combustion, being a trend for decades, releases large amounts of greenhouse gases, contributing to global warming and climate change. This phenomenon is already happening, with observable effects all over the planet, including increasing temperatures, shrinkage of glaciers, decline in coral reefs, changes in crop yield, increase in tree mortality and decrease in tree density, decrease in animal species population, to name a few as reported by the International Panel of Climate Change (IPCC, 2014a) (IPCC, 2014b). With the current behavior in energy consumption, all this effects will be more common with greater impact in the future, with severe consequences for the economy, nature and society. With all this, this phenomenon is one of the biggest threats facing humanity and our environment as we know it, thus it is of vital importance to reduce emissions to the atmosphere by deploying more and better renewable systems for energy consumption.

Solar energy is one source that is helping to the process of migration from fossil fuels, being a clean, sustainable and free source of energy. Both thermal and electric outputs can be obtained directly from the Sun, having big potential for replacing fossil fuels in both thermal process and electricity generation. In order for this to happen, prices and costs of solar energy should keep decreasing so they become more competitive to polluting sources and interesting options for investors and the market. Research and development are essential activities for this process, aiming for better and cheaper technologies or more optimum ways for applying the current ones.

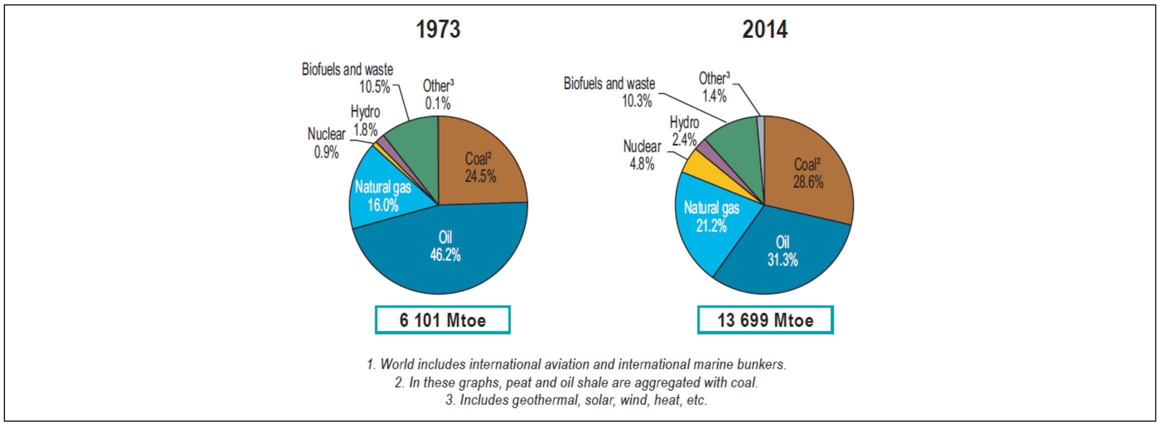

Figure 1.1. Comparison of world primary energy supply by source in 1973 and 2014 (International Energy Agency, 2016)

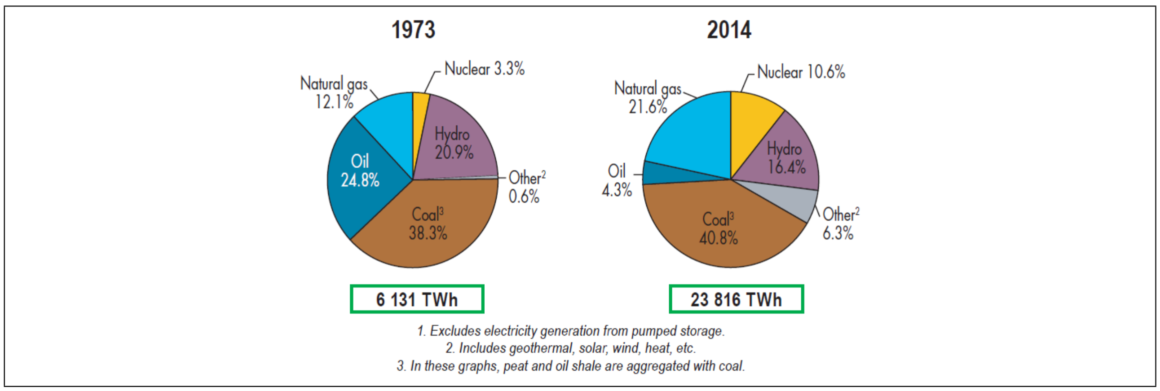

Figure 1.2. Comparison of world electricity generation by source in 1973 and 2014 (International Energy Agency, 2016)

One way to approach this issue is to test different technologies that could give some advantage over the dominant ones, potentially increasing efficiency and lowering costs. Bifacial photovoltaic cells and modules are among these options, nowadays not being use in scale due to the lack of information and testing on performance compared to traditional technologies. Thus, it is vital to perform further testing and research on this technology, looking for improvement aspects and advantages over dominant systems, so it can, potentially, diminish costs and increase deployment.

1.2. Hypothesis and objectives

The hypothesis of this work is that the effects of soiling in the electrical characteristics and performance of bifacial modules are lower than in other photovoltaic technologies.

The objectives of this work are to measure and compare short-circuit current for bifacial and monofacial photovoltaic technologies, study how does soiling affect this parameter and obtain soiling rates for both technologies. Also to develop an optimization tool to find an optimum cleaning frequency for a bifacial photovoltaic system and compare advantages and disadvantages in terms of cleaning and soiling with traditional modules.

1.3. Bifacial solar technology

Bifacial photovoltaic modules can transform solar radiation into electricity from both front and rear sides, unlike traditional solar modules which can only generate power through the front face. This ability has shown to increase electric output consistently between 20% and 30% with the right configuration by changing parameters such as distance to the ground and albedo. The latter is observed in a study carried out by Kreinin et al. (2010), where bifacial modules tilted at 30° with south orientation were installed in a roof top located in Jerusalem, Israel. By varying the distance of the lower edge of the module to the ground, they calculated that power gain due to bifaciality increases from about 5% to over 25% at the largest distance they tested of 108 cm, increasing also short circuit current and improving irradiance distribution in the rear face. They also observed that the power and current gain tends to stabilize with distance, hitting to an optimum at approximately 110 cm in this particular case (Figure 1.3).

In another study by Yusufoglu et al. (2015), the researchers looked at the effects of module elevation, albedo, and reflective area respect to the module area. Through simulations, considering bifacial modules tilted at latitude in Oslo, Norway, and Cairo, Egypt, they observed that the electric output gain depends mainly in the albedo, elevation to the ground and area ratio of the module and reflective surface, as seen in Figure 1.4. From this it can

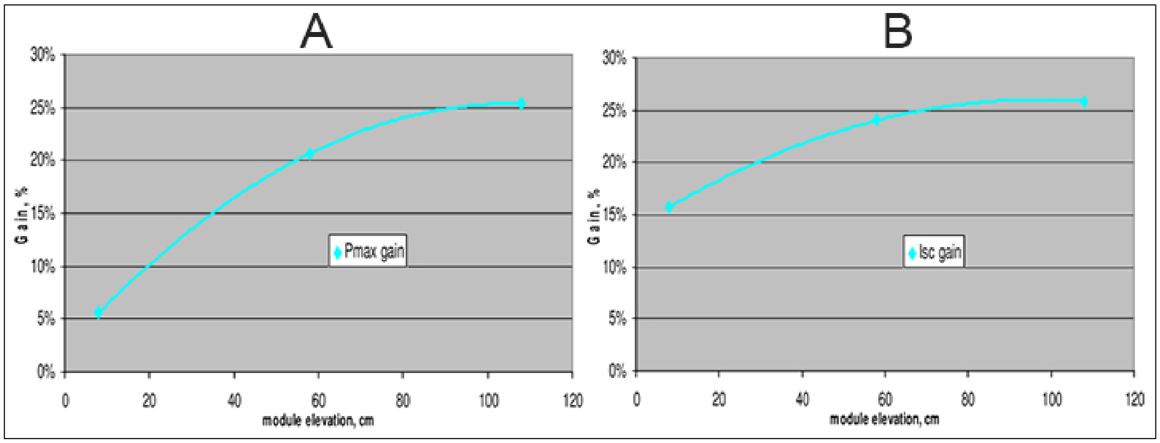

Figure 1.3. P_{max} (A) and I_{sc} (B) gain respect to the module elevation of the surface (Kreinin et al., 2010).

be derived that, for each particular place, there is an optimum configuration depending on this variables, therefore a bifacial photovoltaic systems should be designed considering the above. In other words, designing a photovoltaic system with bifacial modules requires extra analysis compared to traditional technology.

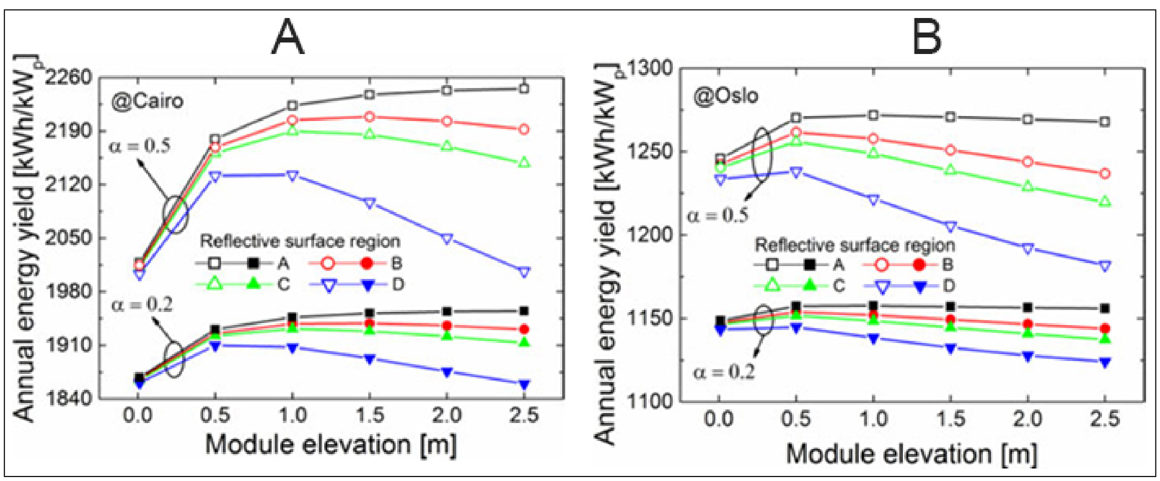

Figure 1.4. Effect of elevation, albedo and reflective area ratio under the module in annual energy yield, for Cairo (A) and Oslo (B). Reflective surface region areas A, B, C and D are 10,000 m^2, 225 m^2, 100 m^2 and 25 m^2 respectively (Yusufoglu et al., 2015).

When designing bifacial systems, it is also important to consider the distance between modules, as shown by Shoukry et al. (2016). The authors simulated a bifacial system of five rows with 11 modules each, varying the row distance d_r from zero to seven meters in two albedo scenarios of 0.2 and 0.5. As seen in Figure 1.5A, the effect of row distance is more noticeable with high albedo, but for both scenarios the bifacial gain BG has negligible change after d_r = 3 m. In particular, when simulating with albedo 0.5 and row distance 2.5 m it can be seen that BG is lower for the center modules and higher for the external ones, being the extremes 27.72 % and 31.20 %.

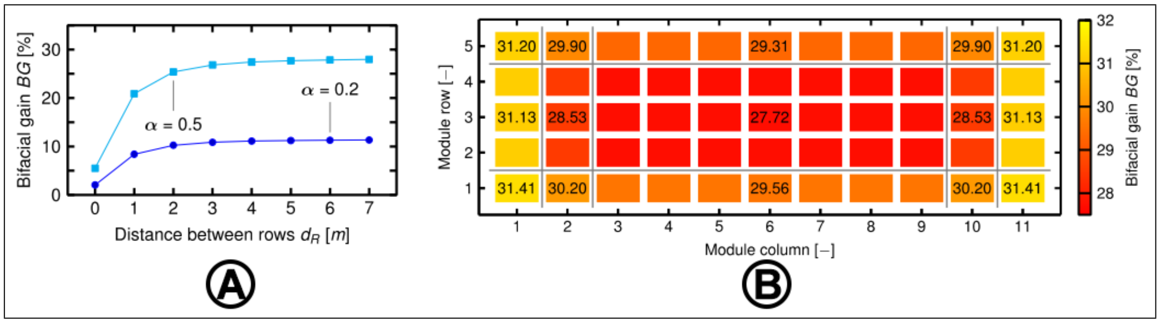

Figure 1.5. Bifacial gain BG relation with albedo and row distance d_r (A). Calculated BG for modules in a PV system with 0.5 albedo d_r = 2.5 m (B) (Shoukry et al., 2016).

One of the main characteristics of bifacial technology is the ability to be installed vertically in an east-west orientation, shifting and splitting the generation peak from mid-day to the morning and afternoon. This configuration could increase the electric production and allow to adjust better to specific demands, depending on albedo and location. This possibility is studied in Obara et al. (2014) for domestic electric demands in Hokkaido region, Japan. The article compares the performance of two simulated hypothetical 1 MW PV plants with battery storage, one with tilted and vertical monofacial modules and the other with vertical bifacial modules with different orientations. They observe that vertical bifacial modules get their generation peak closer to the demand peak, as seen in Figure 1.6. They conclude that, effectively, the electric output from vertical bifacial modules adjusts better to demand, thus allowing to reduce battery storage when using for few households. But, on the other hand, total power generation is reduced compared to monofacial modules, thus when no battery storage is required (i.e: when all the power is consumed considering the complete Hokkaido region demand), no benefit from bifacial modules is observed.

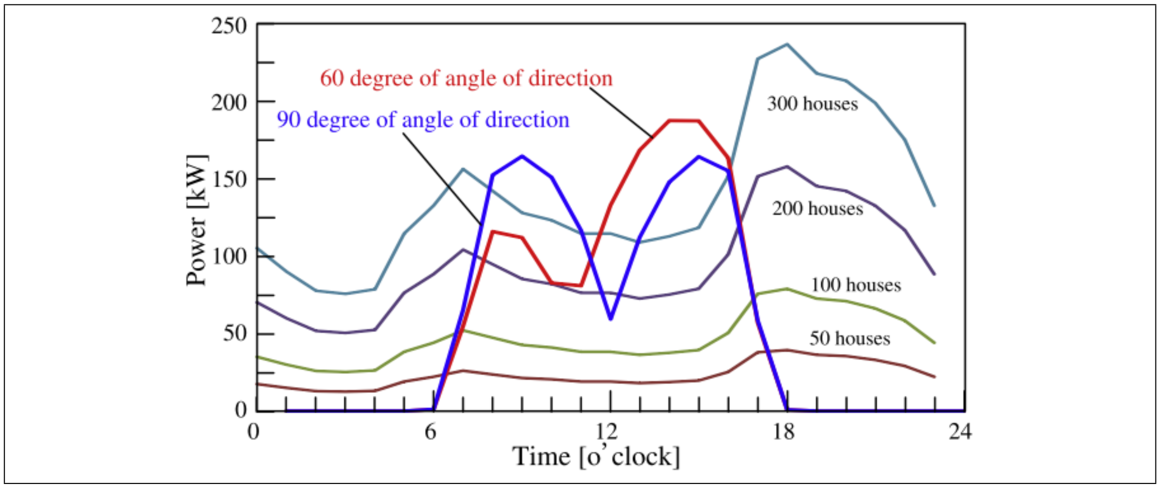

Figure 1.6. Power generation of vertical bifacial module 1 MW plant in the Hokkaido, Japan, and the demand of different number of houses. (Obara et al., 2014)

In a different study, researchers evaluated a 1 kW vertical bifacial grid-connected PV system, with the modules facing west-east (Johnson, Yoon, & Baghzouz, 2012). Along with the outdoor test, the authors performed simulations of irradiance and power generation to compare and validate an analytical model. For irradiance, two pyranometers were installed vertically facing west and east parallel to the modules. For a clear day, they observed discrepancies in both irradiance calculation and power generation, as seen in 1.7. For the irradiance, this differences are mainly due to the structural asymmetry of the location, thus with asymmetric shadows, and due to the miscalculation of the albedo, as the authors report. For the power generation, the biggest difference of the simulated and measured data occurs in the morning, which is attributed to the shading induced by the frame of the modules, reducing by 12% the power output.

To evaluate this further, another study by Siyu Guo et al. (2013), performs the simulation of electric output of vertically mounted bifacial modules and conventionally mounted monofacial modules is compared over the world, considering the different albedo values

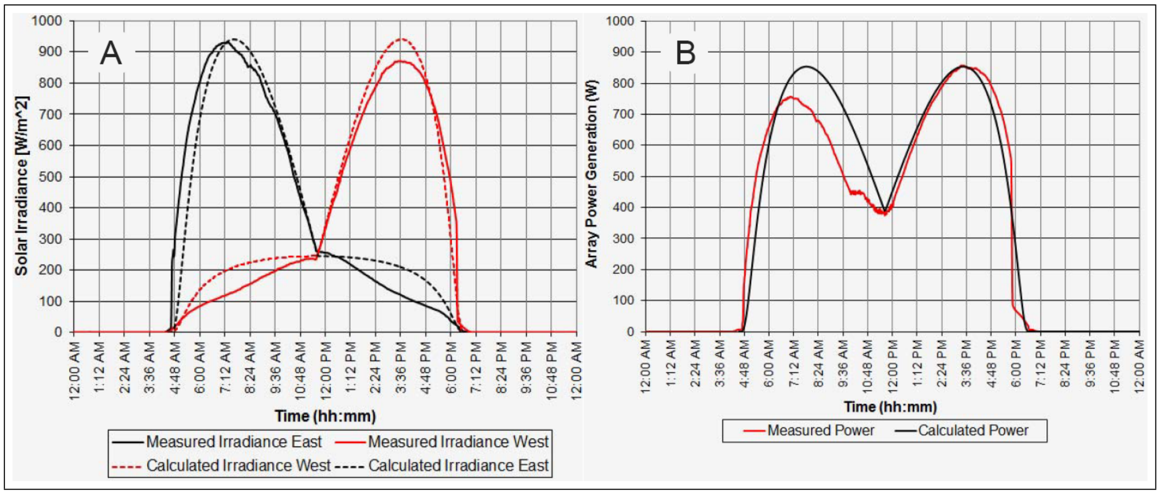

Figure 1.7. Simulated and measured irradiance in west and east facing planes (A) and simulated and measured power for the bifacial PV system (B) (Johnson et al., 2012).

and diffuse fraction in each region. The authors discover that vertical bifacial modules can be more convenient in terms of total electric output than conventional tilted modules in some regions, generally in high latitudes, as seen in Figure 1.8.

1.4. Characterization

Despite of being around for decades and the apparent advantages, market share of bifacial technology is minuscule. Monofacial technology has dominated since the beginning, thus giving bifacial technology low research interest until just the last few years. This lack of interest has dragged a problem unsolved to this day: no standard test conditions for bifacial cells and modules. For traditional solar photovoltaics, standard test conditions (STC) consists basically in illuminating the artifact with a 1000 W/m^2 light, with a 1.5 ATM spectrum at 25°C and measuring the I-V curve.

1.4.1. The I-V curve

The I-V curve of a photovoltaic cell or module plots the behavior between current and voltage output under a particular light condition. The maximum current is obtained when

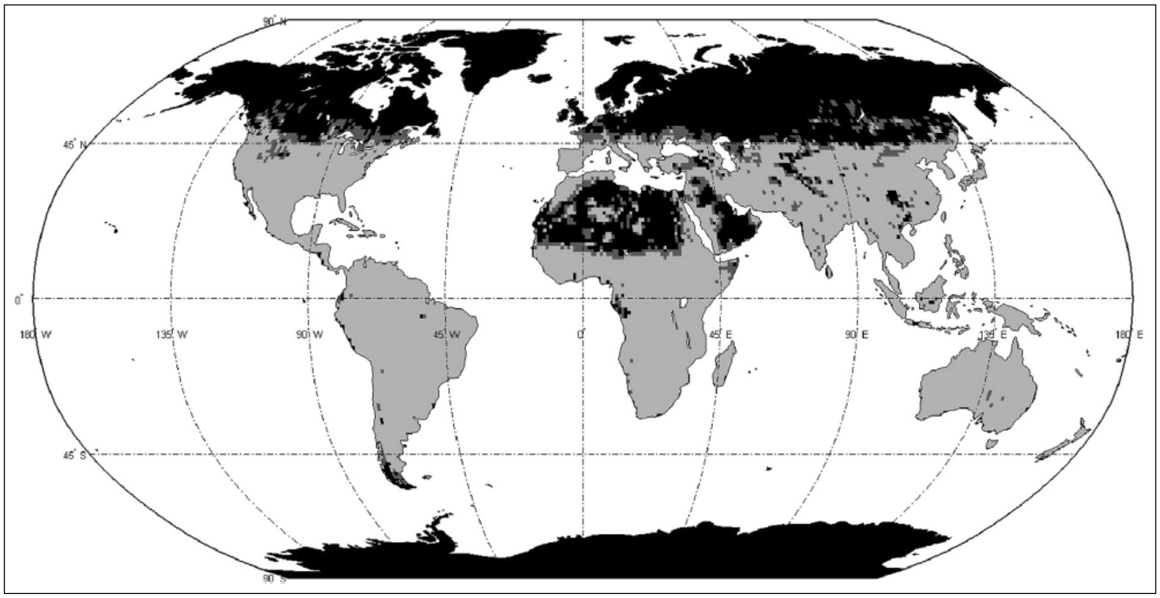

Figure 1.8. Global map indicating where is best to install vertical bifacial modules facing east-west (black) and tilted monofacial modules (light grey) for total power generation. Dark grey indicates similar performance (Guo et al., 2013).

no resistance lays in the circuit, thus called short circuit current (I_{sc}). In this state, voltage is zero. On the other hand, maximum voltage is found when there is an open circuit, thus called open circuit voltage (V_{oc}). In this state, current is zero. The power output of the device is, therefore, the product of the voltage and current at any point of the curve, being the maximum found at the $knee$ of the plot ($P_{max} = I_{mp}V_{mp}$). This curve, also known as the characteristic curve of the device, can be obtained at standard test conditions (STC, 1000 $W/m2$, 1.5 ATM spectrum, 25$°C$). With this curve, it is possible to calculate the efficiency of the device, by dividing P_{max} by the product of the irradiance and the area of the tested item.

To obtain the I-V curve different methods can be applied with different advantages and disadvantages. The easiest way to do this is by a variable resistor. This method consists of a simple circuit containing the device, cell or module, connected in series with a resistor R (Figure 1.10), commonly referred as shunt resistor, capable of varying from 0 to infinity in a series of steps. With the known value R and measuring the potential between its

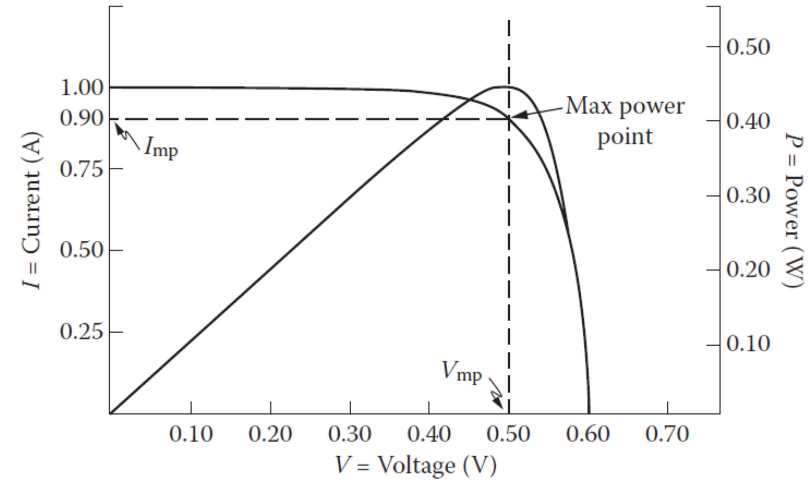

Figure 1.9. Typical I-V curve and power curve of a photovoltaic device. The *knee* of the plot would be where Max power output is found. (Goswami, 2015).

terminals, it is possible to determine the current, thus the curve is obtained by doing this through all the possible values of R.

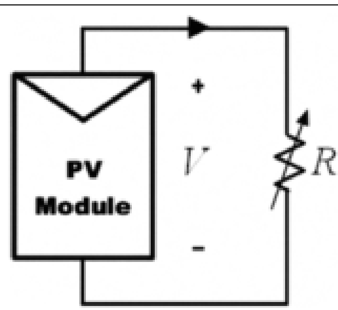

Figure 1.10. Circuit diagram for measuring the I-V curve of a photovoltaic device with a variable shunt resistor (E. Duran et al., 2008).

Though this gives good results for monofacial cells and modules, allowing to make accurate simulations and projections of performance, it gives biased outcomes for bifacial modules and cells since the method assumes electric generation only by the front face of the device. This happens because light will reflect back to the rear side of the cell or module, increasing the power output during the test. In context of the present thesis and for better understanding of the technology, literature review of characterization was performed and classified the papers in bifacial cells and bifacial modules, depending on the focus of the authors.

1.4.2. Bifacial cells

One of the first mentions of this problem was by Mcintosh, Honsber and Wenham (1998), where the authors attempted to measure the effect of rear illumination when characterizing bifacial cells. The main observation by the researchers is that "...it remains clear that the electrical output from a device operating under bifacial illumination cannot be adequately characterized as the sum of its front-only and rear-only electrical output" (McIntosh, Honsberg, & Wenham, 1998). To study this claim further, another publication measured the characteristics of bifacial solar cells (J_{sc} and V_{oc}) using a single light source and mirrors to redirect light into both sides of the cell (Ohtsuka et al., 2001). To simulate different albedo values, they used filters for the incident light of the rear side between the light source and the mirrors. The equipment diagram is shown in Fig. 1.12. When measuring only one side, they covered the other one with a black surface. To interpret the results, they used the following expressions:

$$Separation\ rate(\%) = \frac{J_{sc}(n_f, n_r)}{J_{sc}(n_f, 0) + J_{sc}(0, n_r)} \cdot 100 \tag{1.1}$$

$$\Delta = PM(n_f, n_r) - \Big(PM(n_f, 0) + PM(0, n_r)\Big) \tag{1.2}$$

Where $PM(n_f, n_r)$ is a property, such as V_{oc} or J_{sc}, at n_f suns in the front and n_r suns in the rear side of the cell. The results can be resumed with Fig. 1.11, comparing $J_{sc}(n_f, 0)$, $J_{sc}(0, n_r)$ and $J_{sc}(n_f, n_r)$. In particular, it is noticed that the sum of J_{sc} of each side illuminated separately equals J_{sc} for bifacial illumination. A similar exercise was made for P_{max}, but instead the average of single side illumination would equal bifacial illumination with half of the power (i.e: $P_{max}(n/2, n/2) = \frac{1}{2}[P_{max}(n, 0) + P_{max}(0, n)]$). Overall conclusion is that it is possible to describe J_{sc} of bifacial illumination with the sum of single illumination for each side, contrary to the predictions made by Mcintosh, Honsber and Wenham.

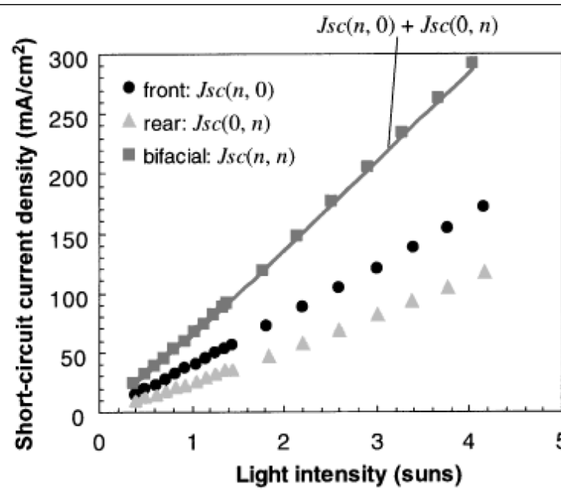

Figure 1.11. Short circuit current density of under bifacial illumination and single front and rear side illumination. Bifacial illumination current density can be obtained by the sum of single side illumination currents. (Ohtsuka et al., 2001)

Another study gets similar results with similar equipment (Ezquer, Petrina, Cuadra, & Lagunas, 2008). The Bifacial Cell Tester (BCT) developed by CENER was used, which consists of mirrors in 45° angle to reflect light from a single source to both sides of a bifacial cell, similar to the one used in (Ohtsuka et al., 2001). Scheme of this device is presented in Fig. 1.12, which uses filters to emulate different albedo values. Using the same notations and equations by Ohtsuka et al., similar results for the separation rate for J_{sc} and V_{oc} are obtained. On the other hand, P_{max} does not follow this trend, as shown in Fig. 1.12 B. At this point is calculated that $\Delta = -0.332\ W$, equivalent to a -19.5% difference for P_{max}.

In a differente study, aiming to determine the influence of bifaciality in STC (Hohl-Ebinger & Warta, 2010), researchers measured the front side current of four different solar cells with seven different chuck surfaces. For this, four equations to estimate the contribution of the rear side were developed:

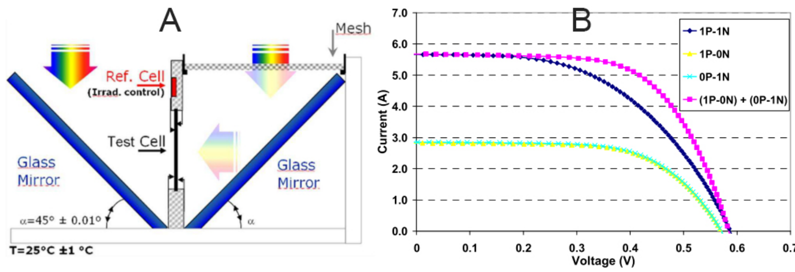

Figure 1.12. Scheme of the apparatus used in (Ezquer et al., 2008), similar to the one used in (Ohtsuka et al., 2001) (A). Comparison between bifacial illumination (1P-1N) and the sum of single side illumination ((1P-0N)+(0P-1N)) for the IV curve (B). (Ezquer et al., 2008)

$$SR_{meas}(\lambda) = SR_{front}(\lambda) + SR_{back,contrib}(\lambda) \tag{1.3}$$

$$= SR_{front}(\lambda) + T_{cell}(\lambda)R_{chuck}(\lambda)SR_{back}(\lambda)$$

$$I_{back,contrib} = \int E(\lambda)T_{cell}(\lambda)R_{chuck}(\lambda)SR(\lambda)\partial\lambda \tag{1.4}$$

$$SR^{rel}_{back,cotrib} = SR_{back,contrib}/SR_{front} \tag{1.5}$$

$$I^{rel}_{sc,back,contrib} = I_{sc,back,contrib}/I_{sc,front} \tag{1.6}$$

Where $SR_{meas}(\lambda)$ is the measured spectral response, $R_{chuck}(\lambda)$ chuck reflectivity, $T_{cell}(\lambda)$ cell transmission, $SR_{front}(\lambda)$ and $SR_{back}(\lambda)$ spectral response of front and back side, $I_{sc,back,contrib}$ back short circuit contribution and $I_{sc,front}$ front short circuit current. Reflectivity of chuck surfaces and transmittance of the cells were characterized. With this information and the described equations, current contribution of the chuck surface was calculated, resulting in a rapid increase with light wavelength above 1,000 nm, and different levels of contributions for each type of cell in different wavelengths, as seen in Fig. 1.13. On the other hand, the integral current contribution gets a maximum valur of 1.07% for Cell B with the gold plated chuck surface, and the lowest value of 0.00% for Cell A with a black plastic foil. It is concluded that, although the contribution can be reduced dramatically, this method could cause a systematic error, overestimating the performance of bifacial solar cells.

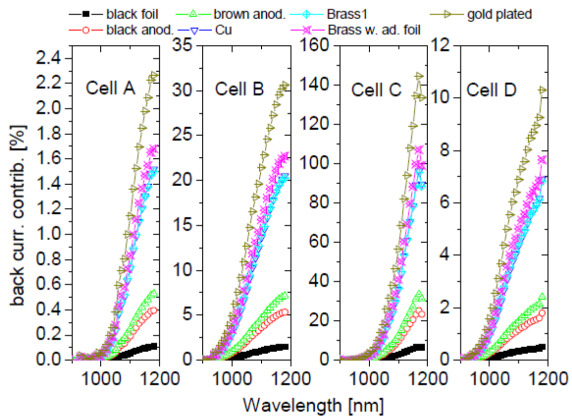

Figure 1.13. Current contribution with different intesities and chuck surface for each cell tested. (Hohl-Ebinger & Warta, 2010)

With a similar approach, (C. Duran, Deuser, Harney, & Buck, 2011) analyzed the influence of chuck reflectivity and cell transmittance on the measurement of the IV curve and internal quantum efficiency (IQE) of the cell. The obtained results are similar, with short circuit current density J_{sc} varying up to 1.01$\%$ for a 85$\%$ reflective chuck surface. Then, bifacial mini modules (one cell modules) with different back sheets were manufactured. They compare the internal quantum efficiency (IQE) the a solar cell v/s the same cell laminated with glass, EVA and a low reflectivity back sheet. It was noticed that wavelengths of 200-400 nm are absorbed by the glass and EVA, while long wavelengths of 900-1200 nm are absorbed by the back sheet, as shown in Fig. 1.14, decreasing the o verall IQE. Also in the same study, a different approach was attempted by illuminating simultaneously both front and rear sides of the cell with different light sources and outdoor measurements of the mini modules. They measured V_{oc}, J_{sc}, fill factor FF and P_{max} for $PM(1,0)$, $PM(1,0.25)$ and $PM(1,0.30)$, for both sides. It was observed that both J_{sc} and P_{max} improved with the amount of illumination, but V_{oc} and FF decreased, with an overall increase of efficiency.

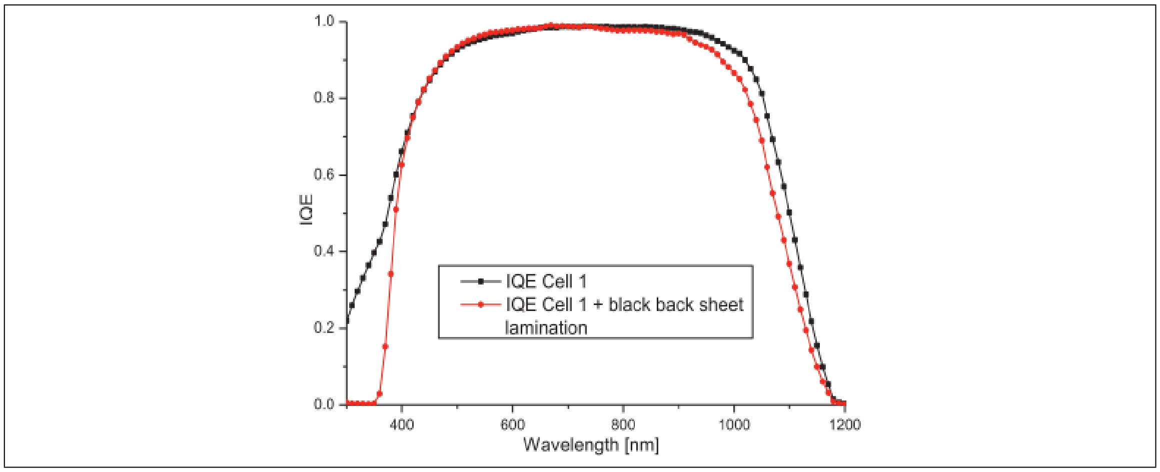

Figure 1.14. Internal quantum efficiency in function of the wavelength for the test cell and the same cell after lamination. (C. Duran, Deuser, et al., 2011)

In a second study carried out by the same author (C. Duran, Hering, Buck, & Peter, 2011), it was performed the same approach obtaining similar results and conclusions when the chuck surface is changed. As in the last investigation, lamination of the cell with different back sheets was made. The illumination results in the cell area and the complete mini module are compared with previous lamination results. Performance of the mini modules increase with the reflectiveness of the back sheet, and also increase when the whole module is illuminated by 8%. A third different experiment its carried out outdoors with small bifacial solar modules, which will be discussed later.

In (Lo, Lim, & Rahman, 2015), indoor measured data is compared with simulated data for bifacial solar cells. The used set-up for indoor measurements considers a light source for both rear and front sides. For each side, simultaneous illumination from 0 to 1 sun were performed, with a total of 24 cases. For the simulations, three programs were used: SMARTS, Radiance and PC1D. This software, together with custom code lines, are integrated with the data simulations. Physical properties of the cell and glass frame such as heat capacity, temperature, conduction coefficient, convection coefficient and radiation coefficient are considered. When IV(0.25,0.50) and IV(1.00,1.00) curves are compared its had the lowest and highest error (RMSE), with 0.09 and 1.43 respectively, as seen in

Fig. 1.15. Similar procedure for bifacial modules is presented in this study, which will be discussed in section 1.4.3.

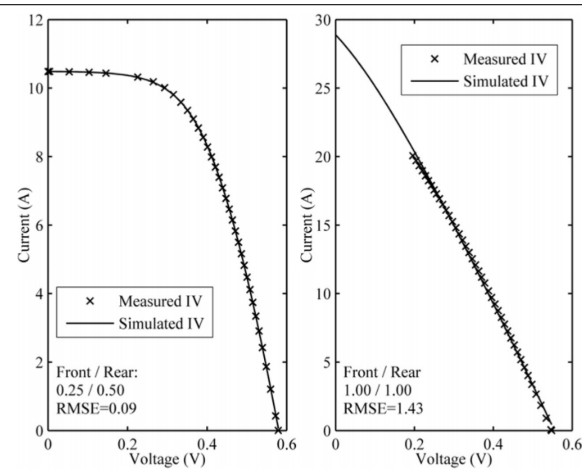

Figure 1.15. Simulated and experimental data compared in IV curve of a bifacial solar cell for different intensity combinations for front and rear.(Lo et al., 2015)

1.4.3. Bifacial modules

With the intention of measuring the efficiency of bifacial modules, four horizontal bifacial modules and four monofacial modules were tested outdoors at 2.4 m from the ground on a pergola (Faiman et al., 2003). The properties of this items are as closely match as possible from the manufacturers data. Two monofacial and bifacial modules are mounted facing down, two facing up. The albedo was measured with monofacial modules with known characteristics, while a pyranometer was used to monitor global irradiance. The efficiency of the bifacial modules was estimated with the following equations:

$$P_u = GA(\eta_f + \alpha\eta_r) \tag{1.7}$$

$$P_d = Ga(\eta_r + \alpha\eta_f) \tag{1.8}$$

$$\eta_f = \frac{(P_u - \alpha P_d)}{(1-\alpha^2)GA} \tag{1.9}$$

$$\eta_r = \frac{(P_d - \alpha P_u)}{(1-\alpha^2)GA} \tag{1.10}$$

Where P_u is the power of the bifacial module facing upwards, P_d facing downwards, G is the global horizontal irradiance, A the cell area, η_f the efficiency of the upward side, η_r of the downward side and α the albedo. For the calculations, it was used albedo and irradiance values of 7 months from May to December in Sede Boquer, Israel (30.87 N, 34.79 E). Results for horizontally mounted modules are shown in Fig. 1.16. For this 7 month trial, the front side efficiency was calculated in 6.0 ± 0.3 % and for the rear side in 4.8 ± 0.2 % for the bifacial module. Also, an effective efficiency was calculated considering the total electric output (front + rear) of the bifacial module for both face-up and face-down modules, resulting in 7.7 ± 0.3 % and 6.9 ± 0.2 %, respectively.

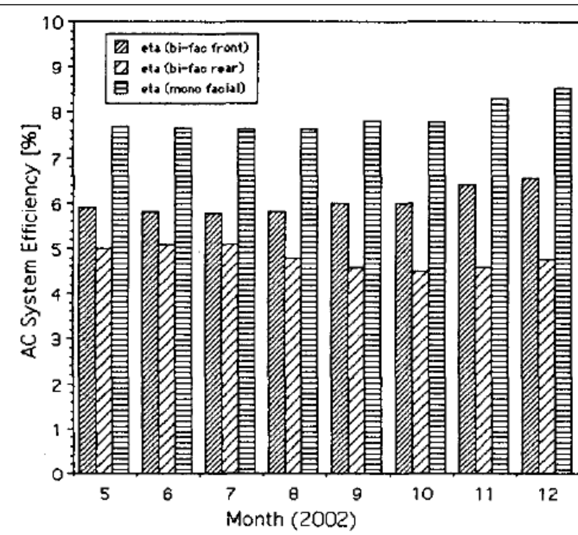

Figure 1.16. Efficiency for horizontally mounted monofacial and bifacial (front and rear) modules. (Faiman et al., 2003)

In (Lo et al., 2015), 2 modules (SP1 and SP2) of 6 bifacial cells in series are tested outdoors horizontally over a mirror surface. Experimental measurements are made during a sunny day and simulation data is obtained using 3 software programs: SMARTS, Radiance and PC1D together with custom code lines. When is compared the measured and simulated IV curves, RMSE are 0.33 and 0.46 for SP1 and SP2 respectively (Fig. 1.17). In particular, daily yield have an error of 17.8% and 18.8% for SP1 and SP2 respectively.

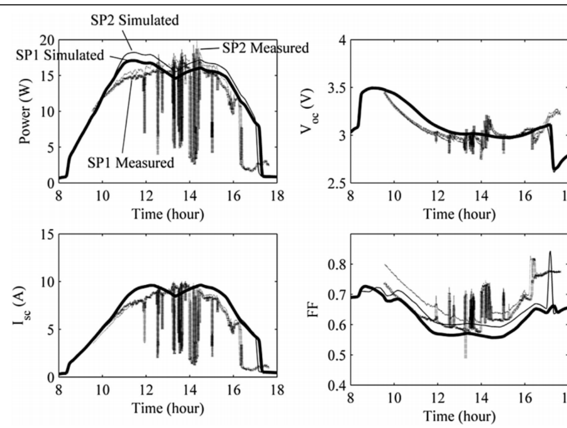

Figure 1.17. Comparison between simulation and experimental data for a particular day. (Lo et al., 2015)

A commercially available bifacial module was tested under STC for monofacial modules (Singh, Aberle, & Walsh, 2014). Single side properties, for both front and rear, where measured by covering the back side with a low reflecting surface (i.e: black cover). V_{oc}, J_{sc}, FF and efficiency for each side where plotted in function of the irradiance, from 200 to 1100 W/m^2. Experimental and simulated efficiency data was compared, as shown in Fig. 1.18. Simulations are obtained by an extensive equation system, but essentially it can be reduced to 3 important equations:

$$P_{bi} = I_{sc-bi} V_{oc-bi} FF_{bi} \tag{1.11}$$

$$\eta_{bi} = \frac{I_{sc-bi} V_{oc-bi} FF_{bi}}{A_{module}(G_f + G_r)} \tag{1.12}$$

$$x = G_r / G_f \tag{1.13}$$

Where A_{module} is the front area of the module, P_{bi},I_{sc-bi},V_{oc-bi} and FF_{bi} the properties of the module under bifacial illumination, G_f and G_r the irradiance in the front a rear side, respectively, and x is the irradiance ratio. This results seem to have good agreement with experimental data. Though, to make the system viable, linear variation of J_{sc} with irradiation is assumed. For the efficiency, there is an absolute difference lower than 0.1% (Fig. 1.18), V_{oc} less than 0.2% and FF 1%.

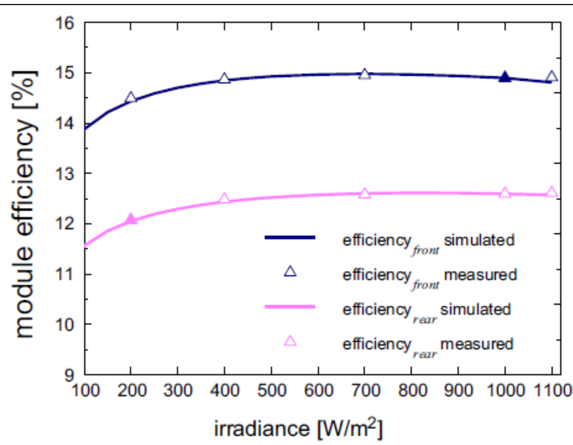

Figure 1.18. Comparison between experimental and simulation data. (Singh et al., 2014)

1.4.4. The characterization problem

After reviewing the articles presented in this section, it can be see that there is a variety of success levels when attempting characterizing bifacial technology. This because no paper seem to have completely nor accurately characterize either bifacial solar cells or modules, though some obtaining good results in particular measurements and variables. Overall, best results are presented in (Lo et al., 2015), and (Singh et al., 2014), accurately simulating indoor controlled measurements of certain properties for bifacial cells. Despite of this, pending work is left for both of this studies, including comparing the simulated bifacial ilumination in (Singh et al., 2014), and study the difference in simulated outdoor performance of bifacial modules in (Lo et al., 2015). Also, an important question rises and remains unanswered with this literature review, whether if $PM(1,1) = PM(1,0) + PM(0,1)$. It is clear that this is true for I_{sc} and Voc, but is unclear if the IV curve or P_{max} should satisfy this equality. Either if the answer is *yes* or *no*, it follows a second question: *why?*. A proper characterization method for bifacial cells and modules should be capable of answering this questions.

1.5. Soiling

Soiling is the accumulation of dust, dirt, snow, or any substance over the photovoltaic module, decreasing its efficiency and therefore reducing the electric output of the system. To fight this effect, regular cleaning of the module's cover is needed, which adds labor, equipment, and water costs. Generally, two types of soiling are recognized: soft and hard soiling. The first makes reference to a film of any substance that reduces the incident irradiance, but still lets light pass through. On the other hand, hard soiling makes references to when the substance, like snow, won't let any light get to the module.

Being a well-known problem, the influence of soiling and it associated expenses have been studied for different photovoltaic and thermal solar technologies in several locations around the world, showing that the results vary for each particular technology, location, climate, season and year (Maghami et al., 2016).

A study by Urrejola et al. (2016), studies module soiling and degradation in Santiago, Chile. The experiment setup consisted in the exposure of monocrystalline, polycrystalline and thin film modules for a period of two years (2015-2016) tilted at a 32° angle and

350° azimuth. All the modules were cleaned monthly during this period. To find soiling and degradation rates of the technologies, performance ratio was used, which compares operation under standard test conditions and real conditions. The results show that soiling rates are different for each technology, season and year. For example, performance ratio decay in autumn for monocrystalline modules was -0.15% daily in 2015, meanwhile in the same season one year later was 2.8 times higher at -0.43%. Overall, thin film has the highest changes in performance ratio due to soiling with a daily average loss of -0.27%, followed by monocrystalline with -0.24% and then polycrystalline with -0.23%.

In another study performed in the same location and with similar approach, researchers aimed to obtain soiling rates and optimal cleaning schedule for a PV system (Besson et al., 2017). In terms of saoiling rate they oberve that decrease i performance ratio varies between 0.19% and 0.83% daily, finding also a correlation with seasonality, being the system less affected in summer months than in winter months, and correlated with concentration of PM10 and PM2.5 particles. Then, to find a optimum cleaning schedule, a mixed integer linear problem was formulated as follows:

$$max \sum_{t=1}^{T} ss_t \cdot CP_t \cdot EP - x_t \cdot CC \tag{1.14}$$

Subject to:

$$ss_{t+1} \leq ss_t - SR_t \cdot (1 - x_t) + x_t + R_t \tag{1.15}$$

$$MinC \leq \sum_{t=1}^{T} x_t \leq MaxC \tag{1.16}$$

$$0 \leq ss_t \leq 1 \tag{1.17}$$

Where the optimized function is the balance between profit and cleaning costs, ss_t is the soiling state, being 100 completely cleaned and 0 completely soiled, x_t the cleaning decision binary variable for each day t, being 1 for cleaning and 0 for not cleaning, CP_t

the daily ideal energy yield not affected by soiling in kWh/day, EP the price at which the energy is sold in USD/kWh, CC the cleaning cost in $USD/kWp/clean$,SR_t the soiling rate in in $\%/day$, R_t a binary variable being 1 if rain is over 1 mm (considered a free perfect cleaning) and 0 for days without rain, $MinC$ and $MaxC$ the minimum and maximum allowed cleanings for the study horizon, t in days, and T as the study horizon in days. The results of the latter are shown in figure 1.19.

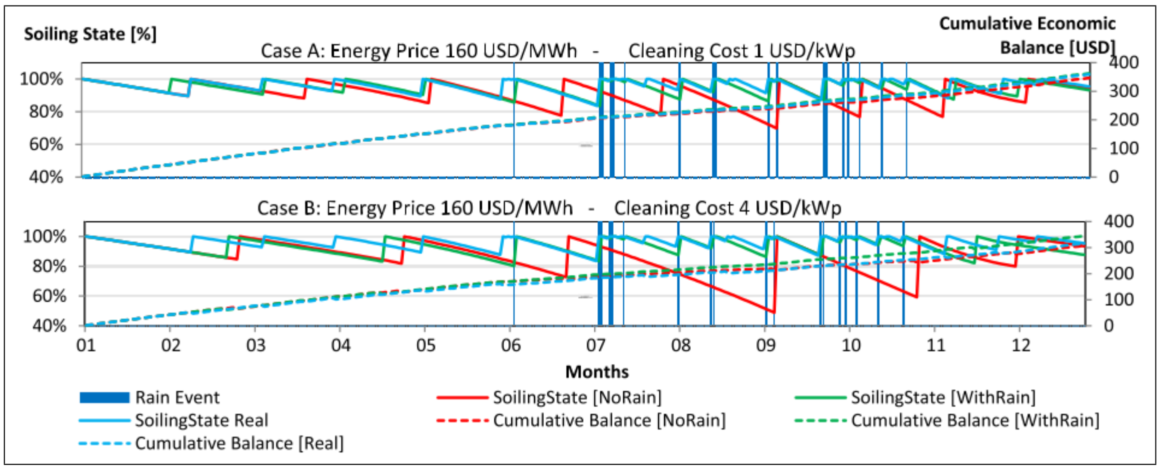

Figure 1.19. (Besson et al., 2017).

Also, it is important to notice that the effects of soiling can vary significantly depending on the local environment. This is very well portrayed in Klimm et al. (2015), where the authors performed a two-yea experiment exposing glass samples at Negev Desert, Israel, and Canary Island, Spain. Visual inspection and analytical analysis was performed, as shown in 1.20. Visually is evident the soiling difference, with different soiling characteristics being more tightly adhered in the maritime environment and more lightly deposited in the dessert climate. Also, there is a vast difference in transmittance after the two-year period, though both samples recovering completely after cleaning.

It is important to mention, that interest in soiling research has increased significantly in the past years, with more papers being published every year. As mentioned by Costa et al. (2016), about 80 papers related to soiling in solar systems were published in 2015, incentivized by the industry interest in solar technology, manufacturing growth, price

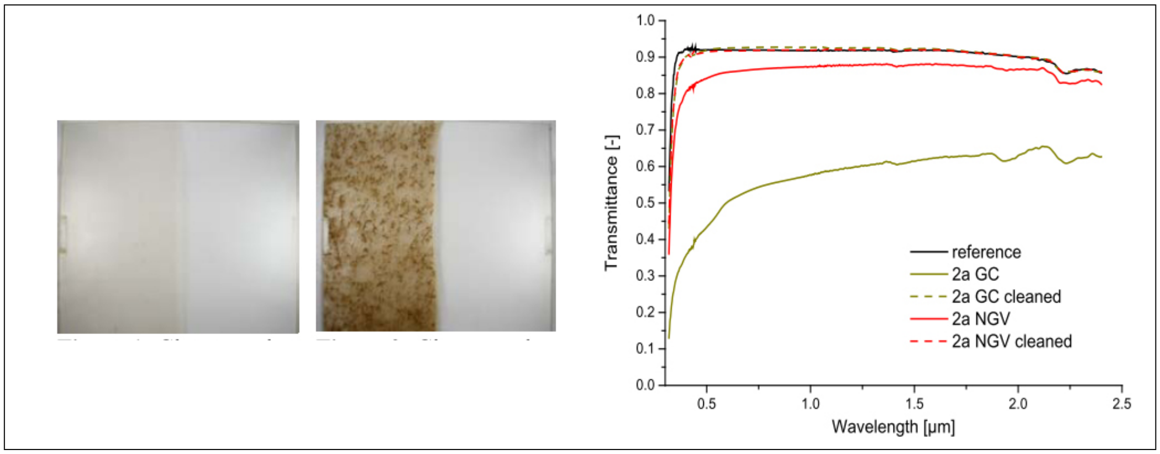

Figure 1.20. (Klimm et al., 2015).

declines and larger number of project deployment. This is illustrated in 1.21, showing a very small group of publications in the early days and significant pump after 2010.

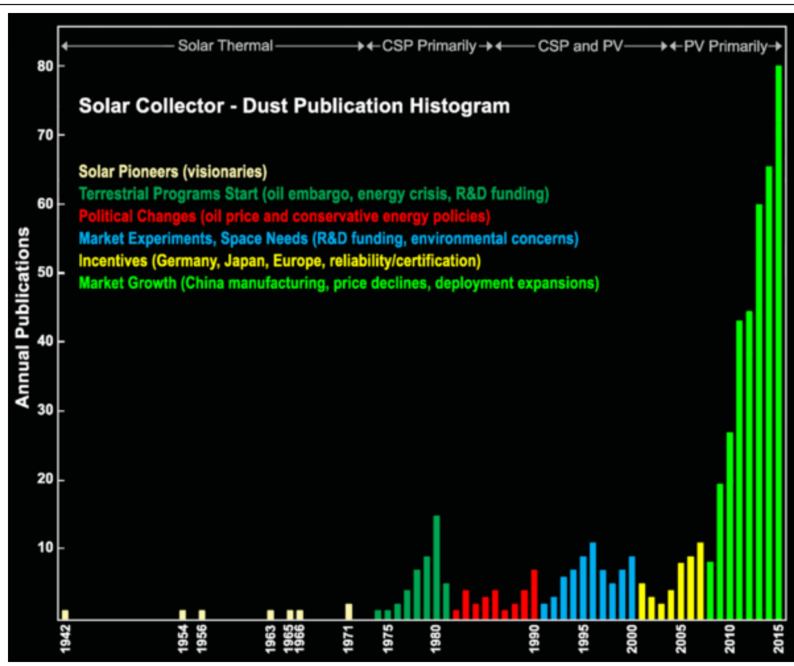

Figure 1.21. Histogram of publications on dust and soiling in solar technology, highlighting driving forces in colors.(Costa et al., 2016).

1.5.1. Soiling in bifacial PV

Despite of being a well-known problem for solar technology, no specific study on soiling for bifacial solar modules has been published to the date of the writing of this work, hence the behavior of this technology under soiling conditions it is not completely understood. It is acknowledged though that soiling diminishes with the angle respect to the horizontal. This is clearly observed in Elminir et al. (2006), where the authors installed glass samples in a roof with different inclinations, from 0° to 90° in 15° intervals, and in different orientations (N, NE, E, SE, S, SW, W and NW). After cleaning monthly during seven months, dust deposition at the 90° tilt angle samples was much inferior than in the other inclinations (Figure 1.22), thus affecting the transmittance of those glass samples less.

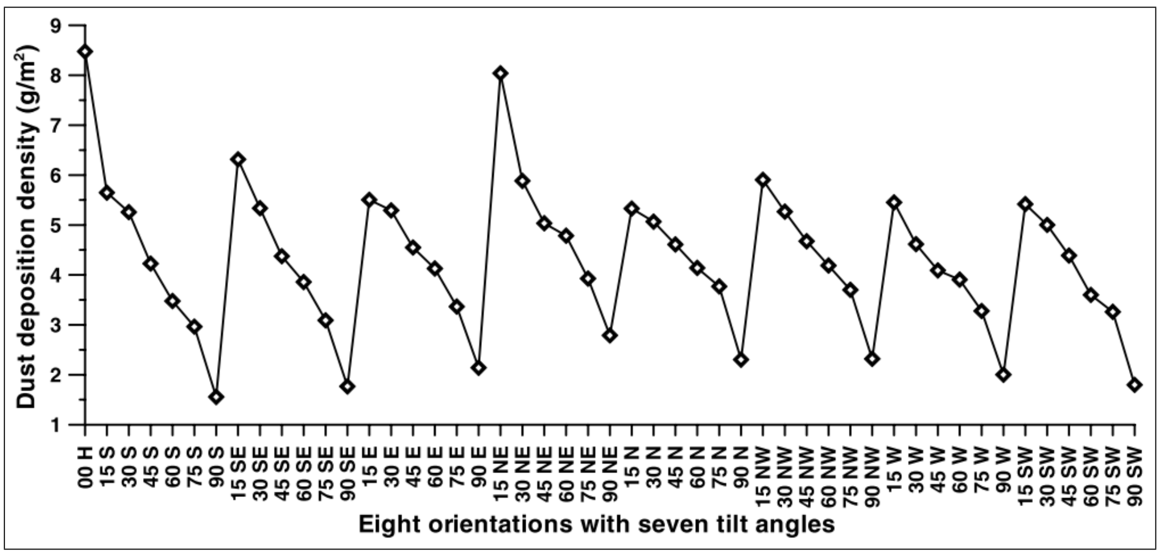

Figure 1.22. Amount of dust accumulation over the glass samples at different inclinations and orientations (Elminir et al., 2006).

Also, in Jiang et al. (2016), a method is develop to estimate dust deposition and cleaning frequency for different particle sizes and module tilts in desert conditions. The developed model is based in the work of You et al. (2012), Zhao and Wu (2006) and Schlichting (1979). Results of the model are shown in 1.23 in logarithmic scale. It can be seen that cleaning time decreases with the increase of particle size and increases with increasing angles. For the latter, when increasing the angle from 0^o to 80^o, the cleaning time goes from 20 to 80 days when particle size in 20 μm, and from 6000 to 25000 days when particle size is 1 μm.

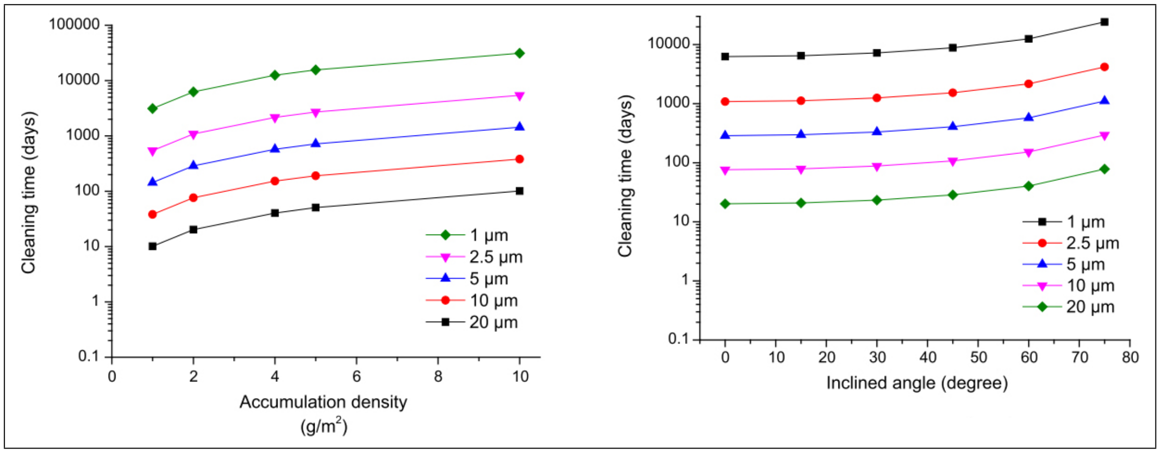

Figure 1.23. (Jiang et al., 2016).

Though there is no specific study in soiling of bifacial modules, there is an interesting observation of this by Hajjar et al. (2016). In this publication, they compare the performance of traditionally installed monofacial modules with vertical bifacial modules in Saudi Arabia. During the experimental period, a dust storm occurred, by which the monofacial modules lost about 60% in performance until they were cleaned, while the bifacial modules didn't show any kind of loss, as seen in Figure 1.24. It must be considered that soiling during dust storms is a very specific situation, thus the results cannot be generalized and extrapolated to other types of dust, soiling and locations. Still, this occurrence is in accordance to the evidence and shows an advantage of vertical bifacial modules.

Another work including soiling in bifacial module study found its a presentation in the 32nd European Photovoltaic Solar Energy Conference and Exhibition (EU PVSEC 2016) in Munich, Germany, during the month of June in 2016. The work aims to see the effects of the structural frame for bifacial modules in energy yield, studying also soiling (Rabanal-arabach, Mrcarica, & Schneider, 2016). The authors installed tilted monofacial and bifacial modules and vertical bifacial modules, measuring short circuit current. After 60 days of outdoor exposition the modules were cleaned. To see soiling effects, they

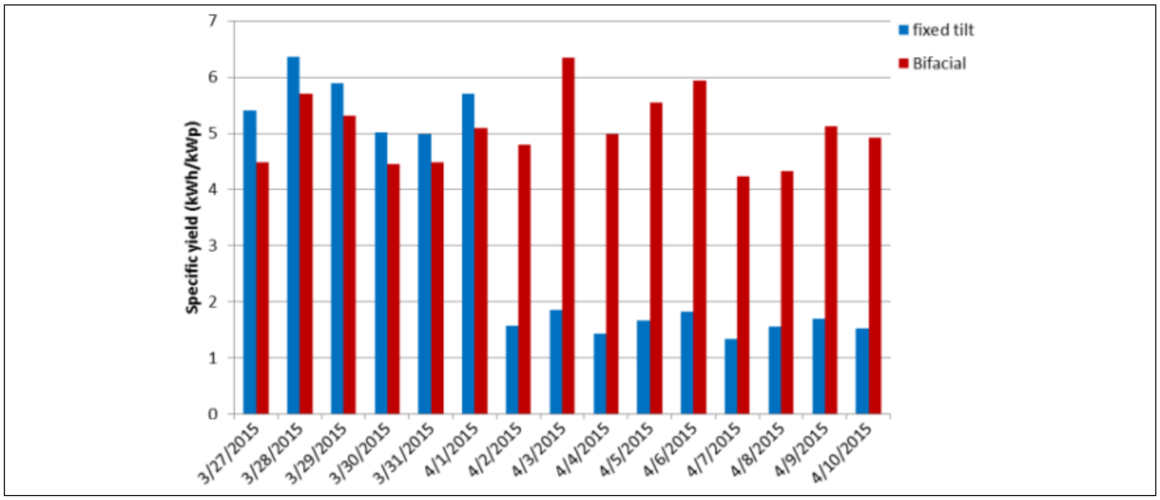

Figure 1.24. Specific yield for vertical bifacial and tilted monofacial modules before and after a sandstorm in Saudi Arabia (Hajjar et al., 2016).

normalized the I_{sc} with global irradiance G_{net}. It is calculated that the difference of this ratio before and after the cleaning is basically 0% for vertical bifacial modules, while the difference for tilted modules were about -12.5% for the bifacial modules and -17.25% for the monofacial module, as showed in Figure 1.25.

Module	Mounting	I_{SC}:G_{net} clean	I_{SC}:G_{net} dusty	Rel. Diff. ($\%_{rel}$)
AR_AR	Tilted	9.34	8.16	-12.63
AR_AR	Vertical	8.78	8.77	-0.11
SM_SM	Tilted	8.81	7.71	-12.49
SM_SM	Vertical	8.45	8.45	0.00
AR_WB	Tilted	7.77	6.43	-17.25

Figure 1.25. Specific yield for vertical bifacial and tilted monofacial modules before and after a sandstorm in Saudi Arabia (Rabanal-arabach et al., 2016).

1.5.2. Effects of soiling in electric characteristics

To better understand the effects of soiling in solar PV technology is important to consider the electric characteristics of the devices. In particular the I-V curve and its components, what will eventually become power and efficiency losses when soiled as seen in the previous section.

Other than reducing the irradiance received by a photovoltaic module, and consequently reducing its efficiency, soiling has effects on the I-V curve, changing the I_{sc}, V_{oc}, P_{max} and its overall shape. This effect is studied by Schill et al. (2015), by monitoring the I-V curve of monocrsytalline modules every five minutes during five months. They observed different effects due to soiling in different climate conditions. Figure 1.26A shows a typical I-V curve for a homogeneously soiled module (September 10). After a small rainfall, the curve shows a slightly different shape due to heterogeneous soiling in the bottom part of the module by accumulation of residue during the rain (September 17). Finally the I-V curve is completely recovered after proper cleaning (September 24). A more drastic effect is observed in a different test site that suffered snow fall, as shown in Figure 1.26B. The soiled I-V curves (open circles) show more clearly the effects of shading, with steps through the curve, though the normal curve is recovered after complete cleaning (closed circles).

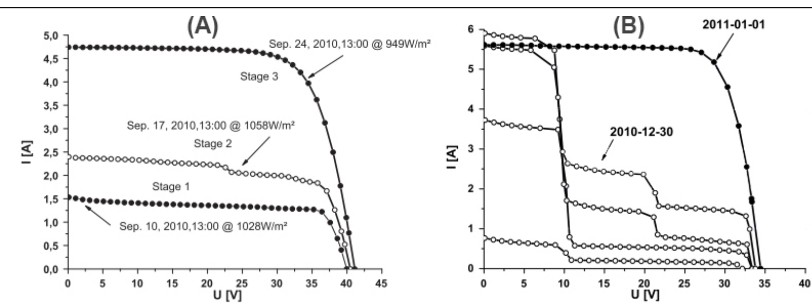

Figure 1.26. (A) I-V curve affected by soiling (September 10), partial shading after minor rainfall (open circles, September 17), and proper cleaning (September 24). (B) I-V curves affected by partial shading because of partial snow coverage (open circles). The snow was gone at the next day (closed circles). (Schill et al., 2015).

On a different study, researchers looked at the effects of different shading situations over the I-V curve of c-Si and p-Si monofacial modules (Dolara, Lazaroiu, Leva, & Manzolini, 2013). For this, they measured the I-V curve while shading a single cell, a cell row (horizontal), cell column (vertical) and diagonally to the module in a series of steps (25%, 50%, 75% and 100%). Though this are shading tests, partial hard soiling can produce this outcomes. The results are show in Figure 1.27 for the c-Si module. Though the shape of the I-V curve is also changed, as observed in the previous study, different overall shapes are obtained. This is explained due to: the particular soiling situation in Schill et al., and the cell grouping per diod of each particular module. In Dolara et al. both c-Si and p-Si modules had three cell groups of 20, and in Schill et al. no diod configuration is described.

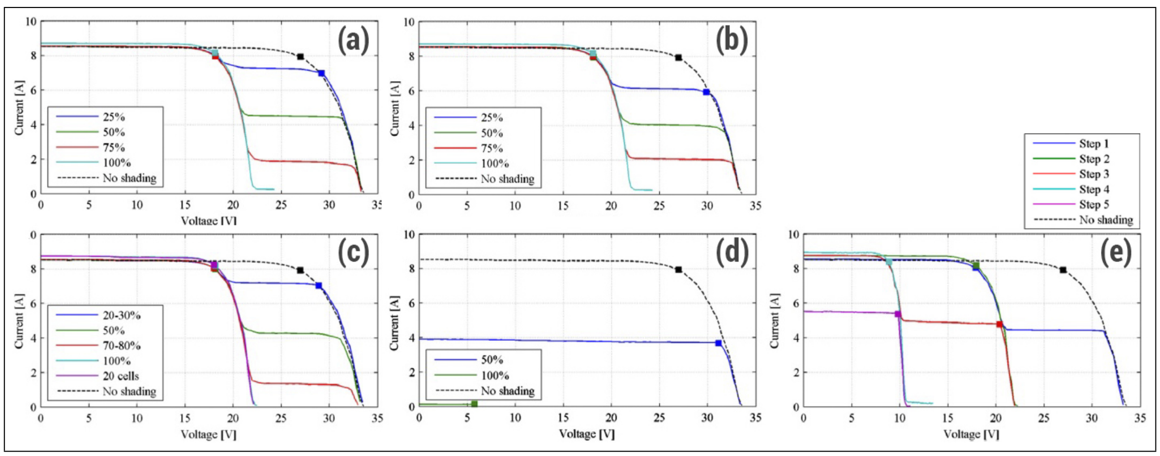

Figure 1.27. I-V profile for different shading situations tested. (a) single cell shading from right to left. (b) single cell shading from bottom to top. (c) cell column vertical shading. (d) cell row horizontal shading. (e) module diagonal shading. Maximum power point are pinned with squares in each curve (Dolara et al., 2013).

In short, it is seen that heterogeneous soiling would change the shape of the IV curve and/or the open circuit voltage V_{oc}, meanwhile homogeneous soiling would change the short circuit current T_{sc}, being proportional to the irradiance (Tan, Tai, & Mok, 2013).

2. ARTICLE

2.1. Introduction

Bifacial photovoltaic (PV) modules can transform solar radiation into electricity from both front and rear sides, unlike traditional solar modules which can only generate power through the front face. This ability has shown to increase electric output with various levels of increment, depending on parameters such as distance to the ground, distance between modules, and albedo (Yusufoglu et al., 2015) (Appelbaum, 2016) (Kreinin et al., 2010). This power gain characteristic has attracted the industry, gaining both commercial and research interest.

Another reason for this growth in engagement with bifacial technology is the capacity to be installed vertically facing east-west. It has been calculated that in this configuration is possible to increase power output compared to a tilted configuration, depending on the geographic location and albedo (Guo et al., 2013). Also, when installed vertically facing east-west the power peak is split in two and shifted to the morning and afternoon, adjusting better to electric demands, lowering storage capacity (Obara et al., 2014).

Even though this technology has been studied since at least the early 60's and scientifically described in the late 70's (Cuevas, Luque, & Ruíz, 1979), research and industry interest has concentrated in monofacial technology, dominating the market with about 97% of the share in 2016, expecting bifacial modules to reach 10% of market share by 2019 and over 35% in 2027 (ITRPV, 2017). This lack of research in those first decades has resulted in a deficient understanding of bifacial devices, making its entrance into the market uncertain and slow. An example of this is the deficient characterization of bifacial cells and modules in Standard Test Conditions (STC). Though the method is accurate and reliable for traditional technology, it has shown not to be adequate for bifacial devices, since the method does not consider bifaciality. Some authors have tried to counter this problem with innovative equipment (Ohtsuka et al., 2001) (Ezquer et al., 2008), but further research is needed to conceive to standard hardware and methodology that outputs reliable and useful information. This characterization problem also lead to a lack of simulation tools for bifacial modules, meaning that it is not possible to generically simulate a bifacial solar system, with some authors developing tools for only particular situations (Lo et al., 2015) (Janssen, Van Aken, Carr, & Mewe, 2015) (Castillo-Aguilella & Hauser, 2016), being a problem for designers and engineers. Though, a recent attempt tried to model generically bifacial systems (Sun, Khan, Deline, & Alam, 2018), considering variables including module elevation, bifaciality and albedo within a comprehensive. To validate their model they compare experimental and simulation results from other published articles including both tilted and vertical mounted bifacial systems. They obtain fairly good results with differences raging from 0.1 to 4.4 percentage points in bifacial gain (i.e: difference between reported bifacial gain in % and calculated bifacial gain in %). Nevertheless, further investigation and development is needed to lower this error and develop a commercial available software that designers can use and that also have better understanding and simulation of degradation (?, ?), thermal effects (?, ?) and proper integration and simulation of albedo (?, ?).

Another matter with lack of research is soiling in bifacial modules. Soiling is the accumulation of dust, dirt, snow, or any substance over the photovoltaic module, decreasing its efficiency and therefore reducing the electric output of the system (?, ?) (?, ?) (?, ?). The influence of soiling and it associated expenses have been studied for different photovoltaic and thermal solar technologies in several locations around the world, showing that the results vary for each particular technology, location, climate, season and year (?, ?).

In terms of bifacial modules, it is known that the accumulation of matter in a surface diminishes with the angle (?, ?), so it is safe to say that bifacial modules will suffer less soiling in the rear side when tilted and in both sides when vertical facing east-west compared to tilted monofacial modules. On the other hand, bifacial modules have two sides to be cleaned, increasing the cost of a complete clean event, compared to monofacial modules. Then it is of vital importance to measure soiling rates for this technology and differentiate between front and rear sides of the bifacial module and optimize cleaning schedules considering all the above.

Only two references were found that included soiling for bifacial modules. The first is in (Hajjar et al., 2016) where they compare the performance of tilted mounted monofacial modules with vertical bifacial modules facing east-west in Saudi Arabia. During the experimental period, a dust storm occurred, by which the monofacial modules lost about 60% in performance until they were cleaned, while the bifacial modules didn't show any kind of loss. It must be considered that soiling during dust storms is a very specific situation, thus the results cannot be generalized and extrapolated to other types of dust, soiling and locations. Still, this occurrence is in accordance to the evidence and shows an advantage of vertical bifacial modules.

Another work including soiling in bifacial modules found aims to see the effects of the structural frame shade in energy yield of bifacial modules, studying also soiling (Rabanal-arabach et al., 2016). The authors installed tilted monofacial and bifacial modules and vertical bifacial modules, measuring short circuit current I_{sc}. After 60 days of outdoor exposure the modules were cleaned. To see soiling effects, they normalized the I_{sc} with global irradiance G_{net}. It is calculated that the difference of this ratio before and after the cleaning is basically 0% for vertical bifacial modules, while the difference for tilted modules were about -12.5% for the bifacial modules and -17.25% for the monofacial module. This work then is also in accordance with evidence and consistent with results observed in Hajjar et al (2016).

This work is focused on soiling analysis for bifacial modules in an attempt to differentiate with traditional PV technology in the matter. For this, a methodology to obtain soiling rates for the rear face from experimental data is proposed, using the information to optimize the cleaning schedule for both front and rear faces of a bifacial PV system, analyzing different scenarios of albedo, cleaning costs, rain and cleaning strategy. The paper is structured as follow: chapter 2 collates the experimental setup and procedure, chapter

3 the optimization model, chapter 4 the results and discussion and eventually, chapter 5 presents the conclusions.

2.2. Experimental setup and procedure

The study was performed on the solar laboratory at Pontificia Universidad Catolica de Chile (PUC). Measurements started on September 12th, 2017 and concluded on November 21st. The modules where tilted at 35^o and 10^o azimuth (North = 0^o).

This study considered two polycrystalline monofacial minimodules and two bifacial monocrystalline minimodules with four cells in series each, as shown in Figure (2.1). For each minimodule, short circuit current I_{sc} was measured through a shunt resistor. Global irradiance in the plane of the array G_{POA} and albedo A were measured with pyranometers. The albedo was measured at 180^o in the same axis as the G_{POA} pyranometer (inverse plane). Data was collected in a time resolution of one minute. An image of the setup is presented in Figure 2.1. For each technology, one module was assigned to be cleaned once a week, while the other was left to soil through the whole experimental period.

Figure 2.1. Experimental setup on the solar laboratory at PUC. On the left a general view of the structure, four modules and pyranometers. At the right a close-up view of the POA and Albedo pyranometers setup.

2.2.1. Data processing

In order to use more representative data, a set of filters were applied to rule out measurements. In particular, the criteria is presented in Table 2.1, as performed in (Besson et al., 2017). With this, days 39 and 51 were ruled completely since radiation in the plane was always under 300 W/m^2 due to heavy cloud density.

Table 2.1. Parameter acceptance criteria for collected data during the experiment period.

Parameter	Acceptance criteria	Unit
G_{POA}	x > 300	$\frac{W}{m^2}$
Solar azimuth	-80 < x < 80	^{o} (North = 0 ^{o})
Solar elevation	x > 25	^{o}

In Figure 2.2, the ratio $R_{IG} = I_{sc,measured}/G_{POA}$ is plotted for each minimodule, being $I_{sc,measured}$ the measured short circuit current, as performed in (Rabanal-Arabach & Schneider, 2016). In Figure 2.3 the relative difference d_r for each technology is shown, defined as

$$d_r = \frac{R_{IG,clean} - R_{IG,soiled}}{R_{IG,clean}} \cdot 100 \tag{2.1}$$

For each technology, d_r is shifted so it is zero for the first day (i.e.: $d_{r,1} = 0$), as shown in Figure 2.3. Comparison between G_{POA} and albedo A and respective averages are presented in Figure 2.4.

2.2.2. Soiling rate

Soiling rate was calculated by subtracting the relative difference in day a ($d_{r,a}$) and day b ($d_{r,b}$), dividing by the number of days $b-a$. Due to rain events, the experiment period was divided in three sections, thus calculating three soiling rates. Between days 19 and 24,

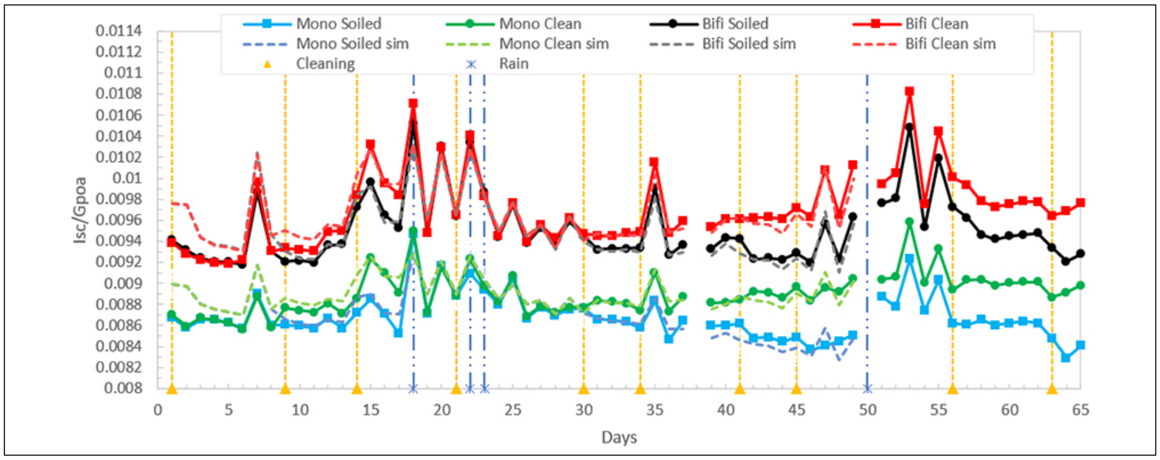

Figure 2.2. Comparison between $R_{IG,soiled}$ and $R_{IG,clean}$ for both monofacial and bifacail minimodules. Dashed lines show the linear regression performed for each set of data.

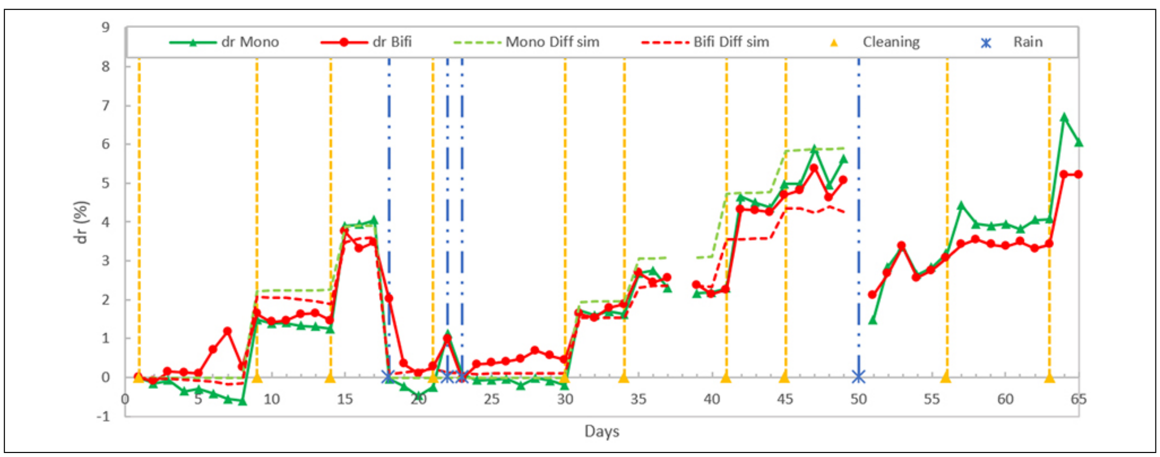

Figure 2.3. Relative difference d_r for both bifacial and monofacial minimodules. Dashed lines show the linear regression performed for each set of data.

heavy rain events cleaned completely the front of all the modules, and a small rain event in day 51 cleaned partially the front of the modules. With the latter, considered periods and respective soiling rates for the bifacial and monofacial minimodules are presented in Table 2.2.

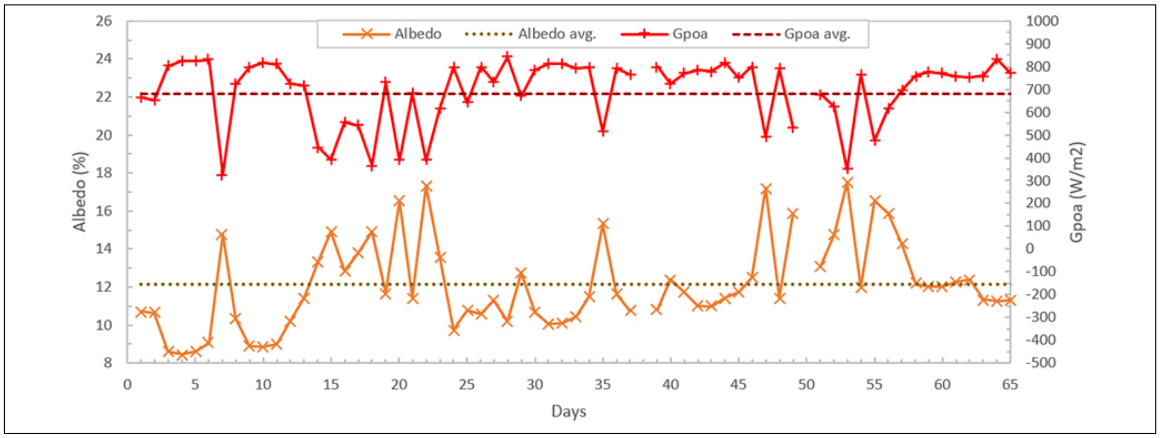

Figure 2.4. Comparison of G_{POA}, albedo A and respective averages.

Table 2.2. Soiling rates for bifacial and monofacial minimodules.

Bifacial minimodule						
Day a	Day b	$d_{r,a}$ (%)	$d_{r,b}$ (%)	$d_{r,b}$ - $d_{r,a}$ (%)	Days	Soiling SR_b $(\%/day)$
1	15	0	3.74	3.74	14	0.249
24	46	0.310	4.81	4.50	22	0.204
51	64	2.13	5.21	3.08	13	0.238
					Average:	0.236

Monofacial minimodule						
Day a	Day b	$d_{r,a}$ (%)	$d_{r,b}$ (%)	$d_{r,b}$ - $d_{r,a}$ (%)	Days	Soiling SR_m $(\%/day)$
1	15	0	3.90	3.90	14	0.279
24	46	-0.0730	4.98	5.05	22	0.223
51	64	1.49	6.71	5.22	13	0.402
					Average:	0.301

To fully characterize soiling in bifacial modules, it should be distinguished between the front and rear faces. For this, it is possible to express the ideal short circuit current of the module I_{sc} as

$$I_{sc} = I_f + I_r \tag{2.2}$$

where I_f and I_r are the ideal short circuit currents contributed by the front and rear sides without soiling, respectively. Also, bifacial modules might have different efficiencies in each side, being the front more efficient than the rear side, then it is possible to write the rear current as

$$I_r = I_f \cdot B \tag{2.3}$$

where B is the bifaciality of the device, defined as

$$B = \eta_r / \eta_f \tag{2.4}$$

being η_f and η_r the efficiency of the front a rear side, respectively. Also, in bifacial devices the rear side receives albedo A, defined as a fraction of the irradiance, so equation 2.2 can be rewritten as

$$I_{sc} = I_f + A \cdot B \cdot I_f \tag{2.5}$$

$$I_f = \frac{I_{sc}}{1 + AB} \tag{2.6}$$

Then, when soiling is present, it is described as a rate in a time scale (day, month, year) multiplied by the time passed since last cleaning, thus:

$$I_{sc,measured} = I_f(1 - SR_f \cdot N_f) + I_r \cdot (1 - SR_r \cdot N_r) \tag{2.7}$$

$$I_{sc,measured} = I_f(1 - SR_f \cdot N_f) + A \cdot B \cdot I_f \cdot (1 - SR_r \cdot N_r) \tag{2.8}$$

$$I_{sc,measured} = \frac{I_{sc}}{1 + A \cdot B}\Big((1 - SR_f \cdot N_f) + A \cdot B \cdot (1 - SR_r \cdot N_r)\Big) \tag{2.9}$$

where SR_f and SR_r are the soiling rates for the front and rear sides of the bifacial module, respectively, N_f and N_r are the time without cleaning for each side, and $I_{sc,measured}$ is the measured current.

To estimate the soiling rate SR_r for the rear side of the bifacial minimodule, experimental data is introduced in equation 2.9 divided by G_{POA} so it is in function of R_{IG} instead of the short circuit current. Soiling rate of the front SR_f is assumed to be equal to the soiling rate of the monofacial module (SR_f=SR_m) and $B = 1$. With the latter, 2.9 is rewritten as

$$R_{IG,measured} = \frac{R_{IG}}{1+A}\Big((1 - SR_f \cdot N_f) + A \cdot (1 - SR_r \cdot N_r)\Big) \tag{2.10}$$

With this, values for SR_r are resumed in Table 2.3. Soiling rates for the bifacial minimodule S_b, monofacial minimodule S_m and for the rear side of the bifacial minimodule S_r are plotted in Figure 2.5.

Table 2.3. Estimated soiling rates for the rear face of the bifacial module

Bifacial minimodule				
Day a	Day b	N_f	N_r	Soiling SR_r $(\%/day)$
1	15	14	14	0.0429
24	46	22	46	0.0357
51	64	13	64	0.396
			Average:	0.0394

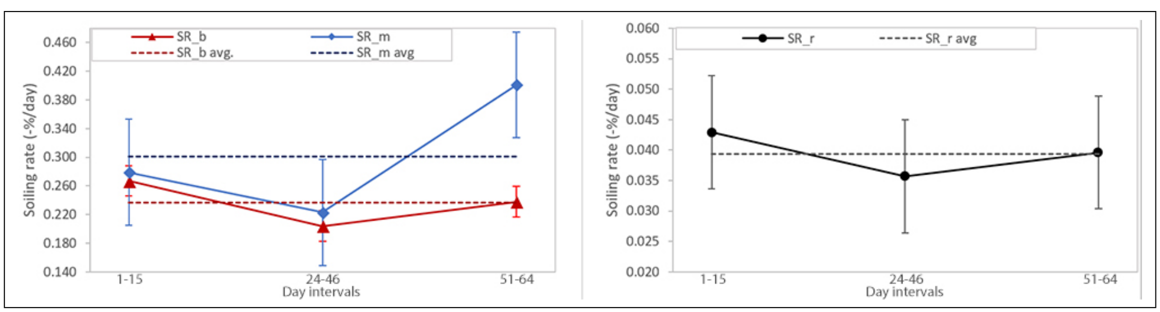

Figure 2.5. Soiling rates during the experimental period for the monofacial and bifacial modules (left) and for the rear side of the bifacial module (right) with respective averages.

2.3. Validation

In order to validate equation 2.10, simulations were performed for the first 49 days introducing experimental data acquired during the experiment. This because the equation supposes known values for N_f and N_r, which was not possible after the rain events in day 50, where the rain cleaned significantly the modules but not completely, thus the equivalent days of soiling is not known.

To estimate the ideal R_{IG} a lineal regression was performed considering only clean days of the bifacial and monofacial modules. Results of the simulations are presented in Figure 2.3 and Figure 2.4 as dashed lines.

To validate the lineal regression, the determination coefficient (R2) was used, as seen in Table 2.4, including also the correlation coefficient and root mean square error (RMSE) as reference. It was obtained a value of 0.84 for both clean and soiled bifacial module R_{IG} (2.2). Also, a 0.89 was obtained for the relative difference, as seen in Figure 2.3. On the other hand, for the clean monofacial a 0.63 value was calculated, meanwhile the relative difference fo the monofacial modules has a 0.94 value.

Table 2.4. Correlation coefficient, R2 coefficient and RMSE for each simulation, between days 1 and 50.

Sim	Corr. Coef.	R2 Coef.	RMSE
Bifi clean	0.91	0.84	0.00013
Bifi soiled	0.91	0.84	0.00014
Bifi diff.	0.94	0.89	0.58
Mono clean	0.79	0.63	0.00012
Mono soiled	0.86	0.75	0.00013
Mono diff.	0.97	0.94	0.63

2.4. Optimization model

The optimization model was based in the approach by Besson et al. (2017). In the publication, they designed an optimization problem for cleaning frequency of a Mono c-Si 1590 W_p system. In particular, what they proposed is the following mixed integer lineal problem:

$$max \sum_{t=1}^{T} ss_t \cdot CP_t \cdot EP - x_t \cdot CC \tag{2.11}$$

Subject to:

$$ss_{t+1} \leq ss_t - SR_t \cdot (1 - x_t) + x_t + R_t \tag{2.12}$$

$$MinC \leq \sum_{t=1}^{T} x_t \leq MaxC \tag{2.13}$$

$$0 \leq ss_t \leq 1 \tag{2.14}$$

Where the maximized function is the balance between electricity cost and cleaning costs, ss_t is the soiling state, being 100 completely cleaned and 0 completely soiled, x_t the cleaning decision binary variable for each day t, being 1 for cleaning and 0 for not cleaning, CP_t the daily ideal energy yield not affected by soiling in kWh/day, EP a constant price of 160 USD/kWh at which the energy is sold, CC the cleaning cost in $USD/kWp/clean$ varying two values of 1 and 4, SR_t the soiling rate in $\%/day$, R_t a binary variable being 1 if rain is over 1 mm (considered a free perfect cleaning) and 0 for days without rain, $MinC$ and $MaxC$ the minimum and maximum allowed cleanings for the study horizon, t in days, and T as the study horizon in days, being 365 for the year 2014.

The latter does not consider bifacaility, so it is necessary to consider it in order to obtain an optimal frequency for bifacial systems. In particular, it is requirement to distinguish between the front and rear face of the bifacial module, thus the problem is modified as follows:

$$max \sum_{t=1}^{T} (ssf_t \cdot CPf_t \cdot + ssr_t \cdot B \cdot A \cdot CPf_t \cdot) EP - CC(xf_t + xr_t) \tag{2.15}$$

Subject to:

$$ssf_{t+1} \leq ssf_t - SRf_t \cdot (1 - xf_t) + xf_t + R_t \tag{2.16}$$

$$ssr_{t+1} \leq ssr_t - SRr_t \cdot (1 - xr_t) + xr_t \tag{2.17}$$

$$MinC \leq \sum_{t=1}^{T} xf_t \leq MaxC \tag{2.18}$$

$$MinC' \leq \sum_{t=1}^{T} xr_t \leq MaxC' \tag{2.19}$$

$$0 \leq ssf_t \leq 1 \tag{2.20}$$

$$0 \leq ssr_t \leq 1 \tag{2.21}$$

where B is the bifaciality of the device, A the albedo, ssf_t and ssr_t are the soiling states for the front a rear sides, CPf_t the ideal energy yield without soiling, xf_t and xr_t the cleaning decision binary variables for each day t and each side, SRf_t and SRr_t the soiling rates in in $\%/day$, $MinC$, $MinC'$, $MaxC$ and $MaxC'$ the minimum and maximum allowed cleanings for the study horizon.

2.4.1. Daily Yield

The daily yield CPf_t was obtained from the simulation of a 1 kWp monofacial system in Santiago, Chile, using the software SAM (National Renewable Energy Laboratory. Golden, 2016) and solar resource data for 2014, 2015 and 2016 measured in the same laboratory as the experiment. From that, CPr_t is in function of CPf_t, this because no reliable enough tool for simulating bifacial systems has been developed, being this a simplistic and deterministic approach for bifacial gain in power yield.

2.4.2. Cleaning Cost

In Besson et. al the CC used is 1 and 4 USD/kW for a low-cost and high-cost cleaning scenarios, respectively. For this work the same procedure was performed, with the additional consideration that the CC is equal for both sides, this because it can not be concluded either a higher or lower value for rear cleaning since no evidence or information on this issue or the is described in the literature. Also it was considered that rain does not affect the soiling state in the rear side, since it is covered by the front and bouncing rain drops from the frame and condensation in the rear side are not accounted to have cleaning effects.

2.4.3. Albedo

During the experiment an albedo value of 0.12 was measured, being the unaltered albedo at the laboratory. Higher albedo magnitudes are fairly common on the literature as in (Yusufoglu et al., 2014) (Shoukry et al., 2016) (Kreinin, Bordin, Karsenty, Drori, & Eisenberg, 2011) (Faiman et al., 2003), so it makes sense to increase the albedo to observe the effects on the model. For this, an albedo of 0.24 is also analyzed, being this the double of the measured albedo in site. Though, 0.24 is easily obtainable with different materials available in nature and the market, as shown in (Brennan, Abramase, Andrews, & Pearce, 2014) with materials such as grey and white shingles, concrete, sandstone, sand and other materials suitable for residential and industrial use.

2.4.4. Electricity Price

In Besson et al., a constant EP of 160 USD/kWh was considered for the one-year optimizations. In this work, as more years were considered, using an average price comes as an important assumption since this costs change every month. In Chile, regulated tariffs are divided in low-tension (BT) and high-tension (AT), having both options different billing schemes and prices for electricity, power and other charges. A common tariff for residential bills is BT-1, which charges only a fixed price (service) and electricity. Taking into account the limitations of this model, as it is more suitable for a small residential system, the BT-1 electricity prices were considered for each month, through 2014 to 2016, for the location of the simulated system at PUC.

2.4.5. Cleaning Strategies

In addition to the latter, different cleaning strategies were evaluated for the bifacial system, being this: separate cleaning (modified model as shown), simultaneous cleaning (by adding restriction 2.22), no cleaning on the rear side (adding restriction 2.23) and cleaning once a month both sides and only the front. A total of 44 analyses were performed for the years 2014 through 2016. Of this 44 cases, 28 are optimizations using the above model and 16 are simulations at steady frequency for once a month (35 cleanings), every two months (17 cleanings), every three months (11 cleanings) and every four months (eight cleanings) for the best case scenario in terms of cleaning costs and albedo of CC=1 USD/kW and $A = 0.12$, as discussed later. The results are summarized in Table 2.5. Lastly, the model was limited to small enough residential systems that can be cleaned in a short time span of at most one day, smallest scale at which the analysis was done.

$$xr_t = xf_t \tag{2.22}$$

$$xr_t = 0 \tag{2.23}$$

2.5. Results and discussion

In this section, results are discussed for the number of optimizations and simulations performed. To ease the latter, each optimization and simulation has been assigned with an identifier consisting in a number and a lower-case letter separated by a dot. When indicating an X instead of the number or letter, it references to all the cases with the explicit character. For example, 7.x indicates all cases that contain 7 (7.a, 7.b and so on), and X.a all cases that contain a (1.a, 2.a and so on) .Every case is referenced to with this nomenclature, which is indicated in Table V as N.

2.5.1. Soiling Rates

In average, soiling rates for the monofacial module was 0.301%/day and for the bifacial module 0.236 %/day, being then the latter 21.6% lower. On the other hand, for the rear side of the bifacial module a soiling rate of 0.0394 %/day was calculated, 7.6 times lower than the front side.

2.5.2. Optimization Cases

As expected, the highest balance was obtained when cleaning cost CC is lower and albedo A is higher, what is seen for each strategy in cases 3.x considering rain and 7.x without rain. On the contrary, the lowest balance was when CC is higher and albedo lower, found in cases 2.x and 6.x. In particular, the highest balance with rain was obtained in case 3.a with \$893 and the lowest in case 2.b and 2.c with \$772, a 13.6% or \$121 lower. This last situation stands out since both 2.b and 2.c have $A = 0.12$ and $CC = 4$, but in 2.b a total of four cleaning events are performed (two in each side), meanwhile in 2.c only one in the front, thus obtaining equal results with less activity. This is illustrated in Figure 2.6A), in addition to simulation 2.a. It can be observed that front cleaning events vary slightly for 2.b, meanwhile 2.a and 2.c present identical cleaning schedule for the front side and 2.a obtaining a \$5 higher balance of \$ 777.

When increasing the albedo from 0.12 to 0.24 and maintaining CC and the strategy, the largest balance gain was observed between 6.b and 8.b of about 12.0% or \$91 with 11 and 12 cleaning in each side, respectively. The lowest increase was observed between 1.c and 3.c of 8.42 % or \$73 with no change in FC (RC = 0). Overall, the average increase in balance by changing the albedo from 0.12 to 0.24 is 10.9 %.

When increasing the cleaning cost CC from 1 to 4 and maintaining albedo and strategy, the largest balance difference was observed between simulations 5.b and 6.b with 12.1 % or \$92 changing FC and RC from 23 to 11, while the lowest difference was found between 3.c and 4.c with 2.65% or \$23 changing FC from 15 to 2 (RC = 0). In comparison, for the monofacial system there is a 3.1% or \$22 difference between 1.e and 2.e changing FC from 15 to 2, and a 9.7% or \$68 difference between 3.e and 4.e changing FC from 34 to 16. For the bifacial system, the average decrease in balance when changing CC from 1 to 4 is 3.2% or \$27 with rain, and 9.3% or \$75 without rain.

When comparing bifacial with monofacial technology it can be appreciated that there are small differences. In fact, when considering rain, the difference in front cleanings is 1 between 1.a and 1.e and no difference between 2.a and 2.e, being the front cleaning frequency virtually the same. In this case, the biggest difference is in the balance values with a 10.4% or \$84 difference between 1.a and 1.e and 10.0% or \$78 difference between 2.a and 2.e. In the same way, without considering rain, the difference lays in the balance, being 10.7% or \$84 higher in 5.a respect to 3.e and both with 34 front cleanings. Also, 6.a is 11.1% or \$79 higher respect to 4.e, but this with the bifacial simulation adds one cleaning over the 16 in 10.b, thus showing a small difference in the three year period considered.

In general, best balance values are obtained when cleaning is optimized separately, followed by simultaneous cleaning being in average 0.57 % lower with rain and 3.2 % without rain. With no rear cleaning the balance is reduced in average 1.5 % with rain and 1.5% without rain. The latter is illustrated in Figure 2.6.C, presenting simulations with same parameters without rain. In the figure, the balance lines show little difference while having significantly different cleaning activities in both front and rear sides. The difference is even lower when rain is present, this because the rain events allow for more similar cleaning schedule on the front face.

Overall, it is clear that albedo has an important effect on the balance value, having a greater effect than the cleaning cost. On the other hand, cleaning costs have a greater effect on frequency, especially when rain is considered. With all this in mind it is evident that, though cleaning the front and rear sides according to the separate cleaning strategy has higher balance values, the difference with simultaneous and no rear cleaning strategies of 0.63 % and 1.5 % (with rain) are low enough that by adding other variables, such as logistics, might turn this results around, since it is easier to schedule a simultaneous cleaning event or just ignore rear cleaning than planing and performing a separate cleaning schedule.

2.5.3. Comparing Optimization with Simulation cases

After the optimizations, simulations of once a month, every two, every three and every four months cleaning was performed for the bets scenario in terms of cleaning costs and albedo of CC=1 USD/kW and $A = 0.12$, and performing cleaning in last day of the corresponding months if daily rain events are under 1 mm during that month. When analyzing the simulation cases it can be seen that for all cases balances are higher when both rear and front cleanings are performed, except for 9.d and 10.d. Also it shows that all optimized scenarios with same CC and A balances are higher. It is interesting to notice simulation 2.d with 15 front cleaning events and 0 rear cleanings, same number as 3.c, but this latter having a balance of \$867 and the first \$862, 0.58% smaller. Just as observed in the optimizations, rain has an important role, reducing necessary cleanings by 63% when optimizing and 53% for the simulations, in average. In terms of balance, 1.d and 3.d have virtually same value of \$881, though the last one with 67% less cleanings. Similarly, 3.d is comparable with 3.b, that with two less cleaning events it obtains a 0.90% smaller balance, and 1.5% smaller than 3.a with one less cleaning event.

Table 2.5. Specifications for each optimization and simulation and number of cleanings events for the front (FC) and rear (RC) and Balance (Bal).

			With rain				No rain			
Tech.	CC ($)	A	N^o	FC	RC	Bal. ($)	N^o	FC	RC	Bal. ($)
Separate cleaning										
Bifi	1	0.12	1.a	16	4	806	5.a	34	3	782
Bifi	4	0.12	2.a	2	1	778	6.a	15	1	709
Bifi	1	0.24	3.a	15	4	894	7.a	33	5	852
Bifi	4	0.24	4.a	2	2	863	8.a	16	2	796
Simultaneous cleaning										
Bifi	1	0.12	1.b	10	10	800	5.b	25	25	760
Bifi	4	0.12	2.b	2	2	774	6.b	12	12	668
Bifi	1	0.24	3.b	10	10	889	7.b	23	23	852
Bifi	4	0.24	4.b	3	3	859	8.b	12	12	759
No rear cleaning										
Bifi	1	0.12	1.c	15	0	797	5.c	33	0	773
Bifi	4	0.12	2.c	2	0	774	6.c	16	0	706
Bifi	1	0.24	3.c	15	0	872	7.c	33	0	848
Bifi	4	0.24	4.c	2	0	849	8.c	15	0	781
Simulations										
Bifi	1	0.24	1.d	15	15	881	9.d	35	35	843
Bifi	1	0.24	2.d	15	0	866	10.d	35	0	846
Bifi	1	0.24	3.d	9	9	881	11.d	17	17	843
Bifi	1	0.24	4.d	9	0	861	12.d	17	0	829
Bifi	1	0.24	5.d	5	5	872	13.d	11	11	818
Bifi	1	0.24	6.d	5	0	854	14.d	11	0	798
Bifi	1	0.24	7.d	4	4	869	15.d	8	8	788
Bifi	1	0.24	8.d	4	0	848	16.d	8	0	767
Monofacial										
Mono	1	-	1.e	15	-	721	3.e	34	-	698
Mono	4	-	2.e	2	-	699	4.e	16	-	630

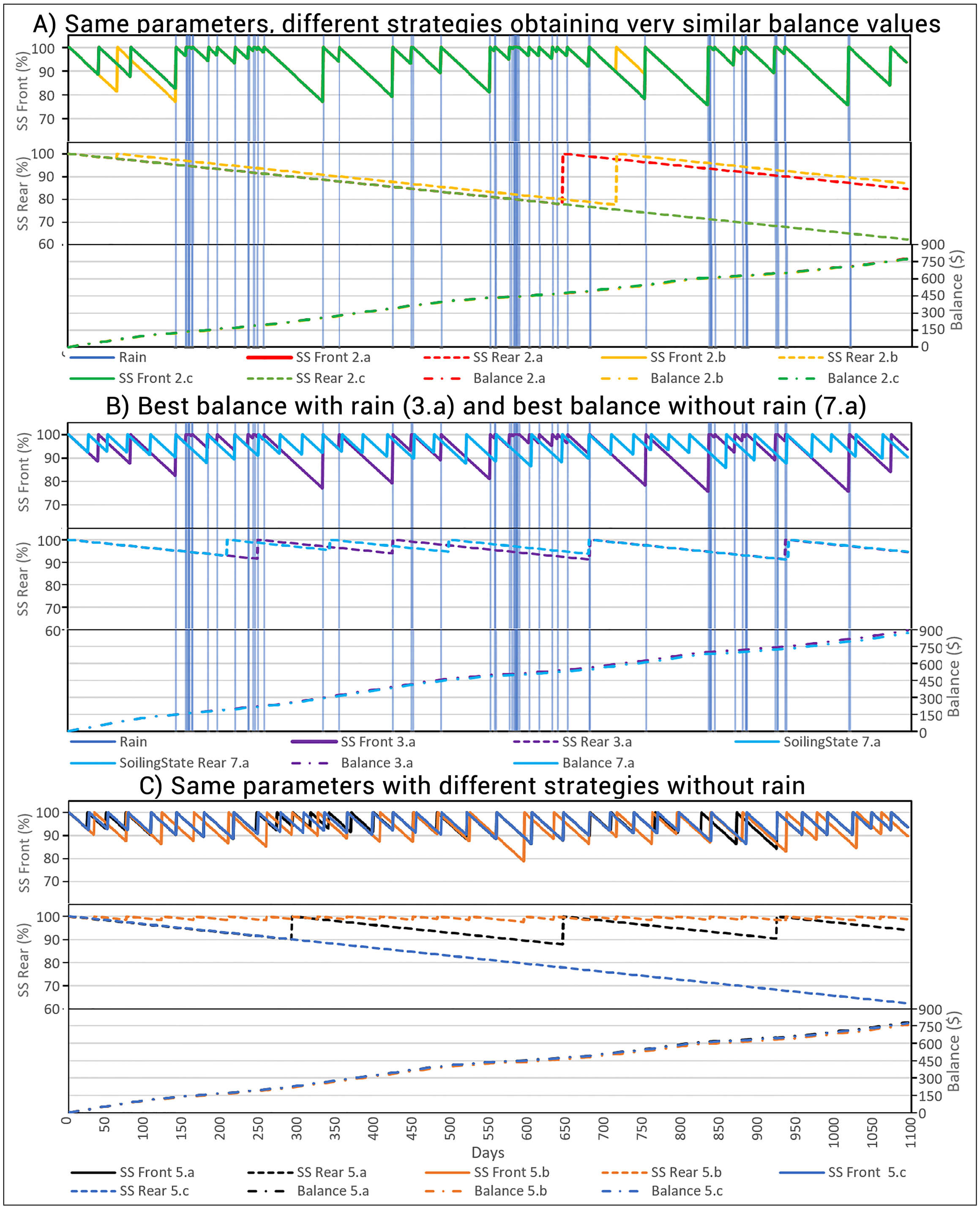

Figure 2.6. Results of optimization model for a sample of optimizations in terms of Soiling State (SS) and Balance. Use Table 2.5 too see exact parameters for each simulation.

2.5.4. Sensibility analysis

When varying the soiling rate SS_r from 0.03 to 0.1 it is seen that, under same cleaning cost CC the balance is always greater for a bifacial system. In the worst case simulated with CC=4, A=0.03 and SS_r=0.104 the balance is \$680, meanwhile the balance for a monofacial system under same conditions is \$667, 1.9% lower. This is due to the particular way on wich the problem is modeled, since bifacility is considered as gain over the monofacial yield, thus always generating more power even if no rear cleanings are performed.

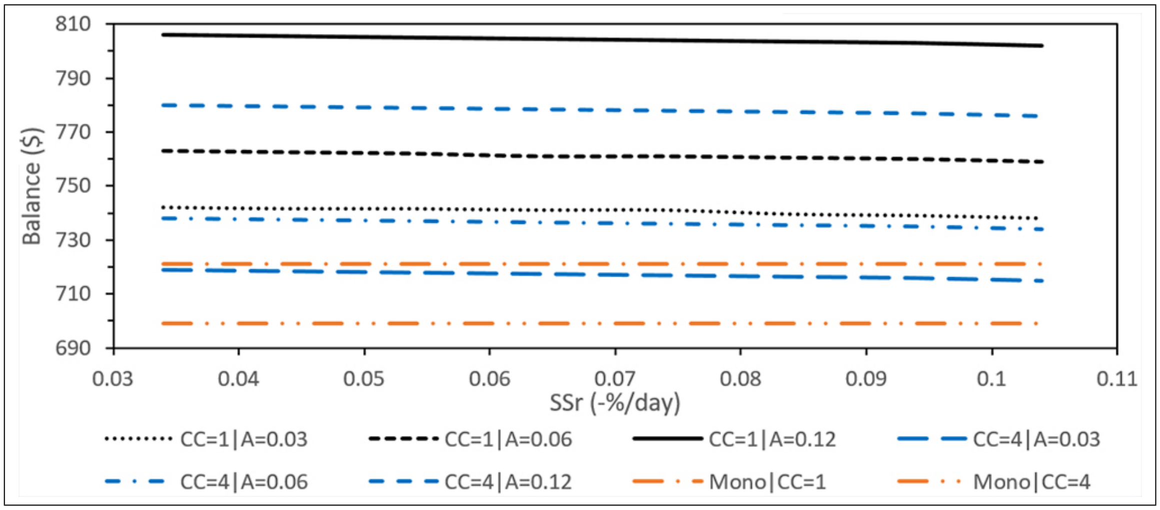

Figure 2.7. Sensibility analisis showing balance with low A values and high soiling rates for the rear face of the bifacial module. Monofacial lines at CC=1 and CC=4 are constant.

2.6. Conclusions

This work analyses the outdoor performance of monocrystalline bifacial mini-modules and polycrystalline monofacial minimodules in terms of soiling by measuring the short circuit current for a period of two months in Santiago, Chile. The main purpose of the investigation was to characterize soiling for bifacial devices and differentiate from traditional technologies. For the latter, a set of equations and methodology are proposed to distinguish soiling on the front and rear sides of the bifacial module. With the equations, average soiling rate of 0.301 %/day is calculated for the monofacial minimodule, meanwhile a rate of 0.236 %/day is estimated for the bifacial module, being then 21.6% lower. For the rear side of the bifacial module a rate of 0.0394 %/day was estimated, roughly 7.6 times smaller compared to the monofacial soiling rate. Then, the equations are simulated using linear regression and soiling data obtained from the two-month period experiment, demonstrating agreement between the simulated and experimental data. Finally, a cleaning optimization model from Besson et al. was modified to consider bifaciality, and several simulations were performed allowing to quantify the effects of albedo, cleaning costs, rain, frequency and strategy in a bifacial system. It is observed that when optimizing for each side separately the balance is greater by less than 3% if is optimized for simultaneous cleaning or without cleaning the rear side at all in a three year period. The small difference suggests that by including other variables into the equation could turn results around, thus ignoring cleaning on the rear side, being already a viable and acceptable strategy under presented conditions and results, might be more profitable in particular situations. When comparing the optimizations with the simulations of simple schedules of 12, six, four and three times a year, it is clear that optimizing is and important exercise, having always better balances in the optimized cases. In general, using the optimization tool decreases the amount of cleaning events and increases balance for the bifacial system, and optimizing rear cleaning separately is the optimum choice of the presented strategies, thus is concluded that soiling in the rear side is an issue that must be considered and studied further.

Acknowledgments

Special thanks to the Energy reseach Centre of the Netherlands (ECN) for providing the monofacial and bifacial minimodules, items with which this work wouldn't have been possible.

REFERENCES

Appelbaum, J. (2016). Bifacial photovoltaic panels field. *Renewable Energy*, *85*, 338–343. doi: 10.1016/j.renene.2015.06.050

Besson, P., Munoz, C., Ramirez-Sagner, G., Salgado, M., Escobar, R., & Platzer, W. (2017). Long-Term Soiling Analysis for Three Photovoltaic Technologies in Santiago Region. *IEEE Journal of Photovoltaics*, *7*(6), 1755–1760. doi: 10.1109/JPHOTOV.2017.2751752

Brennan, M., Abramase, A., Andrews, R., & Pearce, J. (2014). Effects of spectral albedo on solar photovoltaic devices. *Solar Energy Materials and Solar Cells*, *124*, 111–116. doi: 10.1016/j.solmat.2014.01.046

Castillo-Aguilella, J. E., & Hauser, P. S. (2016). Multi-Variable Bifacial Photovoltaic Module Test Results and Best-Fit Annual Bifacial Energy Yield Model. *IEEE Access*, *4*, 498–506. doi: 10.1109/ACCESS.2016.2518399

Costa, S. C., Diniz, A. S. A., & Kazmerski, L. L. (2016). Dust and soiling issues and impacts relating to solar energy systems: Literature review update for 2012-2015. *Renewable and Sustainable Energy Reviews*, *63*, 33–61. doi: 10.1016/j.rser.2016.04.059

Cuevas, A., Luque, A., & Ruíz, J. (1979). Bifacial Transcells for Luminiscent Solar Concentration. In *Electron devices meeting* (pp. 314–317).

Dolara, A., Lazaroiu, G. C., Leva, S., & Manzolini, G. (2013). Experimental investigation of partial shading scenarios on PV (photovoltaic) modules. *Energy*, *55*, 466–475. doi: 10.1016/j.energy.2013.04.009

Duran, C., Deuser, H., Harney, R., & Buck, T. (2011). Approaches to an improved IV and QE characterization of bifacial silicon solar cells and the prediction of their module performance. In *Energy procedia.* doi: 10.1016/j.egypro.2011.06.107

Duran, C., Hering, P., Buck, T., & Peter, K. (2011). Characterization of Bifacial Silicon Solar Cells and Modules: a new step. In *26th european photovoltaic solar energy conference and exhibition.*

Duran, E., Piliougine, M., Sidrach-de Cardona, M., Gala, X, N, J., & Andujar, J. M. (2008). Different methods to obtain the I-V curve of PV modules: A review. *Photovoltaic Specialists Conference, 2008. PVSC '08. 33rd IEEE*, 1–6. doi: 10.1109/PVSC.2008.4922578

Elminir, H. K., Ghitas, A. E., Hamid, R. H., El-Hussainy, F., Beheary, M. M., & Abdel-Moneim, K. M. (2006). Effect of dust on the transparent cover of solar collectors. *Energy Conversion and Management*, *47*(18-19), 3192–3203. doi: 10.1016/j.enconman.2006.02.014

Ezquer, M., Petrina, I., Cuadra, J. M., & Lagunas, A. R. (2008). Design of a Special Set-Up for the I-V Characterization of Bifacial Photovoltaic Solar Cells. *23rd European Photovoltaic Solar Energy Conference and Exhibition*.

Faiman, D., Berman, D., Bukobza, D., Kabalo, S., Karki, I., Medwedt, B., … Oldenkamp, H. (2003). A Field Method for Determining the Efficiency of Each Face of a Bi-facial Photovoltaic Module. *3rd World Conference on Photovoltaic Energy Conversion*. doi: 10.6.02

Goswami, D. Y. (2015). *Principles of Solar Engineering, Third Edition* (Third ed., Vol. 1). Boca Raton, FL: CRC Press. doi: 10.1017/CBO9781107415324.004

Guo, S., Walsh, T. M., & Peters, M. (2013, nov). Vertically mounted bifacial photovoltaic modules: A global analysis. *Energy*, *61*, 447–454. doi: 10.1016/j.energy.2013.08.040

Hajjar, H., Dubaikel, F., & Ballard, I. (2016, apr). Bifacial photovoltaic technology for the oil and gas industry. *2015 Saudi Arabia Smart Grid, SASG 2015*. doi: 10.1109/SASG.2015.7449283

Hohl-Ebinger, J., & Warta, W. (2010). Bifacial Solar Cells in STC Measurement. *Proceedings of the 25th European Photovoltaic Solar Energy Conference*.

International Energy Agency. (2016). *Key World Energy Statistics* (Tech. Rep.). Paris, France: International Energy Agency. doi: 10.1787/key_energ_stat-2016-en

IPCC. (2014a). *Climate Change 2014: Impacts, Adaptation, and Vulnerability. Part A: Global and Sectoral Aspects. Contribution of Working Group II to the Fifth Assessment Report of the Intergovernmental Panel on Climate Change [Field, C.B., V.R. Barros, D.J.*

Dokken, K.J. (Tech. Rep.). Cambridge, United Kingdom and New York, NY, USA: Cambridge University Press.

IPCC. (2014b). *Climate Change 2014: Impacts, Adaptation, and Vulnerability. Part B: Regional Aspects. Contribution of Working Group II to the Fifth Assessment Report of the Intergovernmental Panel on Climate Change [Barros, V.R., C.B. Field, D.J. Dokken, M.D. Mastrandre* (Tech. Rep. No. 1). Cambridge, United Kingdom and New York, NY, USA: Cambridge University Press. doi: 10.1007/s13398-014-0173-7.2

ITRPV. (2017). *International Technology Roadmap for Photovoltaic Seventh Edition, March 2017* (Tech. Rep. No. Eighth Edition). Frankfurt, Germany. Retrieved from `http://scholar.google.com/scholar?hl=en{&}btnG=Search{&}q=intitle:International+Technology+Roadmap+for+Photovoltaic{#}1` doi: http://www.itrs.net/Links/2013ITRS/2013Chapters/2013Litho.pdf

Janssen, G. J., Van Aken, B. B., Carr, A. J., & Mewe, A. A. (2015). Outdoor Performance of Bifacial Modules by Measurements and Modelling. *Energy Procedia*, *77*, 364–373. doi: 10.1016/j.egypro.2015.07.051

Jiang, Y., Lu, L., & Lu, H. (2016). A novel model to estimate the cleaning frequency for dirty solar photovoltaic (PV) modules in desert environment. *Solar Energy*, *140*. doi: 10.1016/j.solener.2016.11.016

Johnson, J., Yoon, D., & Baghzouz, Y. (2012). Modeling and analysis of a bifacial grid-connected photovoltaic system. *IEEE Power and Energy Society General Meeting*. doi: 10.1109/PESGM.2012.6345266

Klimm, E., Kaltenbach, T., Philipp, D., Masche, M., Weiss, K.-a., & Koehl, M. (2015). Soiling and Abrasion Testing of Surfaces for Solar Energy Systems Adapted to Extreme Climatic Conditions. *Pvsec 31*(September), 1–3.

Kreinin, L., Bordin, N., Karsenty, A., Drori, A., & Eisenberg, N. (2011). Outdoor evaluation of power output improvement of the bifacial module. In *Conference record of the ieee photovoltaic specialists conference.* doi: 10.1109/PVSC.2011.6186308

Kreinin, L., Bordin, N., Karsenty, A., Drori, A., Grobgeld, D., & Eisenberg, N. (2010).

PV Module Power Gain due to Bifacial Design. Premliminary Experimental and Data.

Lo, C. K., Lim, Y. S., & Rahman, F. A. (2015). New integrated simulation tool for the optimum design of bifacial solar panel with re fl ectors on a specific site. *Renewable Energy*, *81*.

McIntosh, K., Honsberg, C., & Wenham, S. (1998). The Impact of Rear Illumination on Bifacial Solar Cells with Floating Junction Passivation. In *2nd world conference on photovoltaic solar energy conversion* (pp. 1515–1518).

National Renewable Energy Laboratory. Golden, C. (2016). *System Advisor Model Version 2016.3.14 (SAM 2016.3.14).* Retrieved from `https://sam.nrel.gov/content/downloads.`

Obara, S., Konno, D., Utsugi, Y., & Morel, J. (2014). Analysis of output power and capacity reduction in electrical storage facilities by peak shift control of PV system with bifacial modules. *Applied Energy*, *128*, 35–48. doi: 10.1016/j.apenergy.2014.04.053

Ohtsuka, H., Sakamoto, M., Koyama, M., Tsutsui, K., Uematsu, T., & Yazawa, Y. (2001). Characteristics of bifacial solar cells under bifacial illumination with various intensity levels. *Progress in Photovoltaics: Research and Applications*. doi: 10.1002/pip.336

Rabanal-arabach, J., Mrcarica, M., & Schneider, A. (2016). The Need of Frameless Mounting Structures for Vertical Mounting of Bifacial PV Modules. In *32nd eu pvsec.* Munich, Germany. doi: 10.4229/EUPVSEC20162016-5CO.14.5

Rabanal-Arabach, J., & Schneider, A. (2016). Anti-reflective Coated Glass and its Impact on Bifacial Modules' Temperature in Desert Locations. *Energy Procedia*, *92*, 590–599. doi: 10.1016/j.egypro.2016.07.024

Schill, C., Brachmann, S., & Koehl, M. (2015). Impact of soiling on IV-curves and efficiency of PV-modules. *Solar Energy*, *112*, 259–262. doi: 10.1016/j.solener.2014.12.003

Shoukry, I., Libal, J., Kopecek, R., Wefringhaus, E., & Werner, J. (2016). Modelling of Bifacial Gain for Stand-alone and in-field Installed Bifacial PV Modules. *Energy Procedia*, *92*, 600–608. doi: 10.1016/j.egypro.2016.07.025

Singh, J. P., Aberle, A. G., & Walsh, T. M. (2014). Electrical characterization method for bifacial photovoltaic modules. *Solar Energy Materials and Solar Cells*, *127*, 136–142. doi: 10.1016/j.solmat.2014.04.017

Sun, X., Khan, M. R., Deline, C., & Alam, M. A. (2018). Optimization and performance of bifacial solar modules: A global perspective. *Applied Energy*, *212*(September 2017), 1601–1610. doi: 10.1016/j.apenergy.2017.12.041

Tan, R. H. G., Tai, P. L. J., & Mok, V. H. (2013). Solar Irradiance Estimation Based on Photovoltaic Module Short Circuit Current Measurement. *IEEE International Conference on Smart Instrumentation, Measurement and Applications (ICSIMA)*(November), 26–27.

Yusufoglu, U. A., Lee, T. H., Pletzer, T. M., Halm, A., Koduvelikulathu, L. J., Comparotto, C., … Kurz, H. (2014). Simulation of energy production by bifacial modules with revision of ground reflection. *Energy Procedia*, *55*, 389–395. doi: 10.1016/j.egypro.2014.08.111

Yusufoglu, U. A., Pletzer, T. M., Koduvelikulathu, L. J., Comparotto, C., Kopecek, R., & Kurz, H. (2015, jan). Analysis of the annual performance of bifacial modules and optimization methods. *IEEE Journal of Photovoltaics*, *5*(1), 320–328. doi: 10.1109/JPHOTOV.2014.2364406